

FUJI ELECTRIC REVIEW

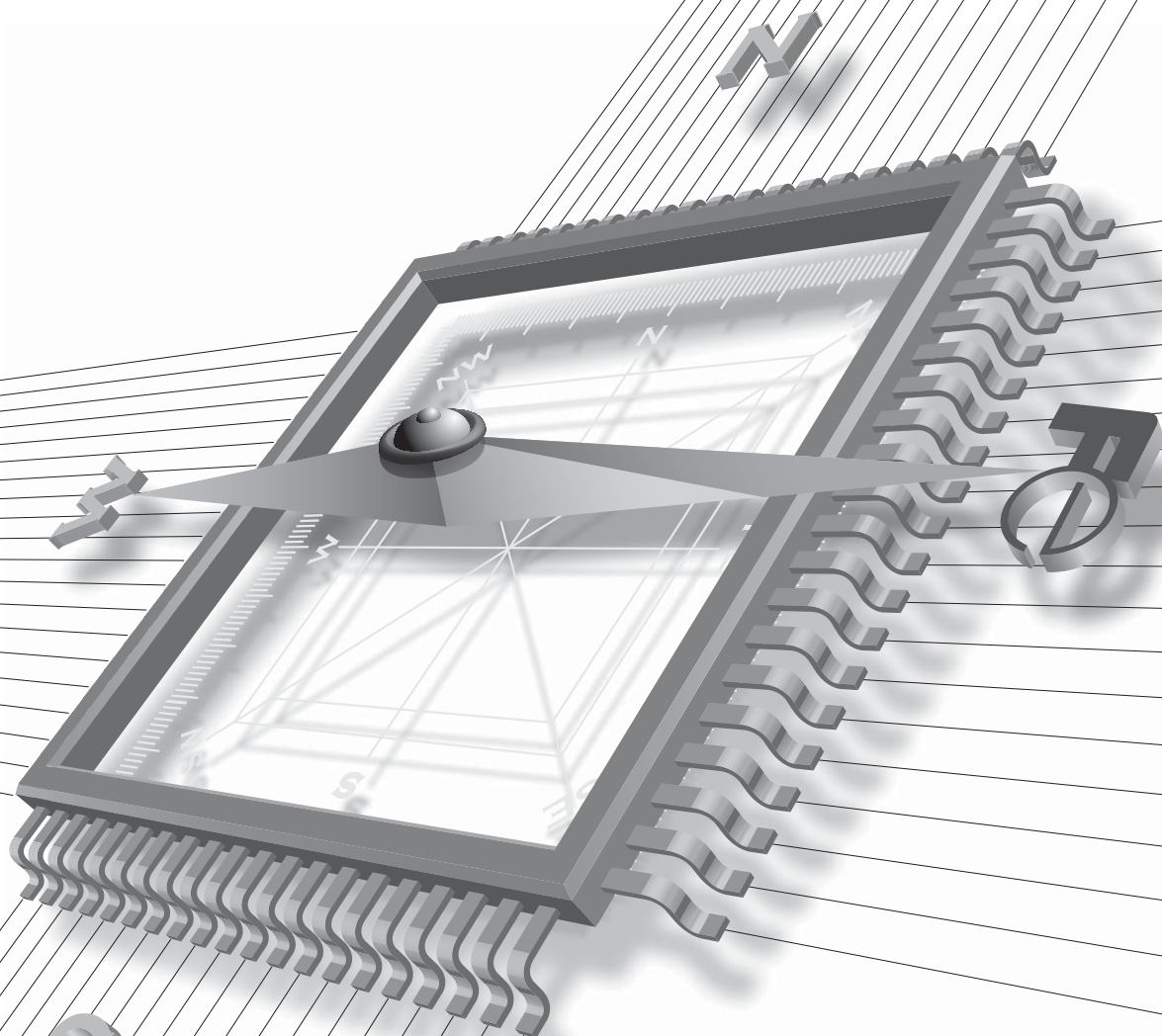
Semiconductors

3

2007 VOL.53



Fuji Electric Group



A way forward for systems

Fuji Electric's power devices are the lifeblood of power electronics.

Fuji Electric Device Technology is a group of professionals providing capable support to leading-edge businesses.

Our job is to provide solutions for our clients and the marketplace.

■ **"New Dual" U4 series IGBT module**

Realizes low loss and small size at the world's highest level.

■ **Econo-IPM**

Intelligent power module equipped with overheat protection function.

■ **IGBT-IPM**

Realizes world's first all-silicon construction, houses leading-edge chips.



Fuji Electric's Power Devices

FUJI ELECTRIC REVIEW

Semiconductors

3

2007 VOL.53

CONTENTS

Fuji Electric's Semiconductors: Current Status and Future Outlook	60
IGBT Modules for Electric Hybrid Vehicles	65
New Concept IGBT-PIM Using Advanced Technologies	69
All Lead-free IGBT Modules and IPMs	73
Development of Pressure Sensor Cell for Fuel Leak Detection	77
M-Power 2A Series of Multi-chip Power Devices	81
Multi-output PDP Scan Driver IC	85
A 2nd Generation Micro DC-DC Converter	89

Cover photo:

The development of semiconductors for automotive use gained momentum with the trend beginning in the 1980s toward greater use of electronics in automobiles, and many types of sensors and microcomputers have been used in such applications. Recently, out of concern for the global environment and in order to conserve energy, there has been a rapid increase in the application of semiconductors to engine and cruise control systems.

Fuji Electric has developed such products as high performance MOS FETs, power ICs, one-chip igniters and pressure sensors to contribute to the higher performance of automobiles. Additionally, Fuji Electric has optimized for automobile use its proprietary high voltage and large current capacity IGBTs to develop a hybrid vehicle IGBT-IPM (intelligent power module).

The cover photo shows IGBT-IPMs developed for application to automobiles.

Fuji Electric's Semiconductors: Current Status and Future Outlook

Tatsuhiko Fujihira
Hisao Shigekane

1. Introduction

The June 1, 2006 issue of “nature” reported⁽¹⁾ the results of an investigation of deposits on the North Pole ocean floor indicating that the ocean surface temperature at the North Pole approximately 55 million years ago was about 23°C, which is 10°C or more higher than had been previously estimated by meteorological simulations. The expanding global economy and growing population are driving an increase in energy consumption and CO₂ emissions⁽²⁾, and unless this trend is slowed, serious impact from the greenhouse effect is a concern⁽³⁾. The abovementioned article in “nature” indicates that the predicted greenhouse effect and its impact might be reconsidered for the worse, and that the limiting of CO₂ emissions is a more important issue for mankind.

All member companies of the Fuji Electric Group, whose corporate mission includes “seeking harmony with nature”, have been working to protect the global environment through providing products and technologies that contribute to the conservation of the global environment, reducing the environmental burden over the course of a product's lifecycle, and promoting business activities that also reduce environmental burden as part of Fuji Electric's basic corporate policy. Fuji Electric especially focused on the business areas of power electronics, which aims to utilize electric power energy effectively, and power semiconductor devices, the main components in this field, as businesses whose contribution is crucial to protecting the global environment. Electric power accounts for more than 40 % of primary energy, and since this percentage is expected⁽²⁾ to increase unilaterally, power electronics and power semiconductor devices will be expected to become even more important in the future.

Power semiconductor devices help to protect the global environment and in particular, to reduce CO₂ emissions by increasing the efficiency with which electric power is used, thus contributing to resource conservation (miniaturization) and to expanding the usage (by lowering the cost and expanding the range of applications) of power electronic equipment. In particular, the specific performance of power semiconduc-

tor devices themselves must be improved, control and sensing functions must be enhanced to realize better performance, smaller size, higher reliability and lower cost, and the lineup and applications of power semiconductor products must be expanded.

This paper describes the current status and future outlook for Fuji Electric's representative semiconductor products: power modules, power discretes and power ICs.

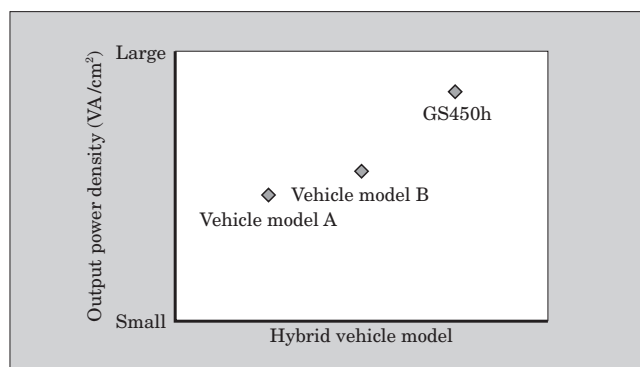
2. Power Modules

Fuji Electric's recent major accomplishments involving power module products are the mass-production of IGBT (insulated gate bipolar transistor)-IPMs (intelligent power module) for use in hybrid vehicles and the market launch of the U4 series of IGBT modules.

As is explained in detail in this issue, last year for the first time, Fuji Electric's IGBT-IPM is being utilized in the PCU (power control unit) of a hybrid vehicle, and is being mass-produced. The vehicle model is the LEXUS*¹ GS450h, and we take pride in the acceptance of Fuji Electric's proprietary technology to realize high power, low loss, small size and high reliability in

*1: LEXUS is a registered trademark of the Toyota Motor Corporation.

Fig.1 Comparison by car model of output power density (IPM output power / IPM base area) of hybrid vehicle-use DC-DC converter IPM

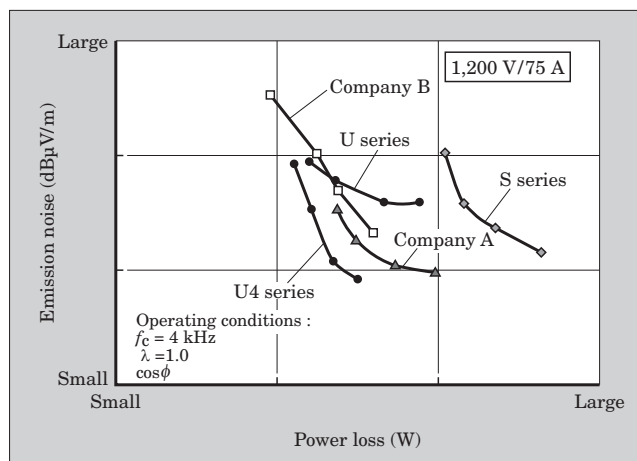


the global LEXUS brand of hybrid cars that feature rapid acceleration, good fuel economy, excellent design and high quality. Figure 1 shows a comparison with the output power density (IPM output power per IPM base area) of conventional IPMs used in a DC-DC converter for the same application. It can be seen that the output power density has been improved dramatically compared to that of the IPMs used in vehicle models A and B. The use of the U series IGBT chip set that incorporates Fuji Electric's proprietary technology⁽⁴⁾⁽⁵⁾ to realize low loss, high durability and small size, and the design of a package optimized for the particular application contribute to the dramatic improvement in output power density. This IPM uses an alumina DCB (direct copper bonding) + Cu base structure to realize high heat dissipation and high reliability⁽⁶⁾, and is the world's first application of this structure to an automotive IPM, successfully realizing a dramatic decrease in cost. Also, the use of Fuji Electric's independently developed lead-free solder has resulted in the world's first all lead-free automotive IPM.

The U4 series of IGBT modules were developed based on Fuji Electric's U series technology, and realize a higher carrier frequency and lower noise emission. The U4 series is effective in industrial-use motor driver applications for increasing the carrier frequency while suppressing emission noise and conduction noise⁽⁷⁾. Figure 2 compares the tradeoff between emission noise and power loss, as measured on a Fuji Electric test bench while varying the gate resistor, for the U4 and other series. The U series, characterized by ultra-low loss, was very effective in reducing inverter loss, but was difficult to use because adjustment of the gate resistor and optimization of the main circuit wiring were sometimes required in order to reduce noise. The U4 series enables a significant reduction in noise to be achieved through adjustment of the gate resistor only, and is extremely easy to use.

6th generation V series IGBT modules have been developed for release at the end of fiscal 2006. With

Fig.2 Comparison of the tradeoff between emission noise and power loss measured by varying the gate resistor



an improved FS (field stop) structure and trench gate structure to realize significantly lower loss and smaller size than the U series, and the incorporation of low noise technology acquired during development of the U4 series, the V series is expected to be easy to use, even for noise reduction.

2006 was the year in which RoHS^{*2} compliance and lead-free implementation of power modules was achieved. All new products are already RoHS-compliant, and existing products have been made fully RoHS-compliant and lead-free during 2006.

Fuji Electric is advancing the development⁽⁸⁾ of higher reliability and higher heat dissipating packages, MOS (metal oxide semiconductor) gate type conduction modulation devices and SiC devices, and plans to introduce them in this journal within several years.

3. Power Discretes

Low voltage MOSFETs (MOS field effect transistors) are one of the main types of power discretes, and in 2005, Fuji Electric began mass-producing a 2nd generation trench MOSFET. Figure 3 shows a cross section of this MOSFET structure. By integrating Fuji Electric's proprietary quasi-plane junction technology and drain ballast resistance technology with trench technology, the specific on-resistance per unit area was reduced by approximately 20 % and the $R_{on} \cdot Q_{gd}$ figure of merit was improved by approximately 30 % while ensuring the same level of short-circuit withstand capability and avalanche tolerance as a 1st generation device.

Fuji Electric's main power discrete products are the Super FAP-G series⁽⁹⁾ of high voltage MOSFETs, the high voltage SBD (Schottky barrier diode) series

*2: RoHS is restriction of the use of certain hazardous substances in electrical and electronic equipment.

Fig.3 Cross section of 2nd generation trench MOSFET structure

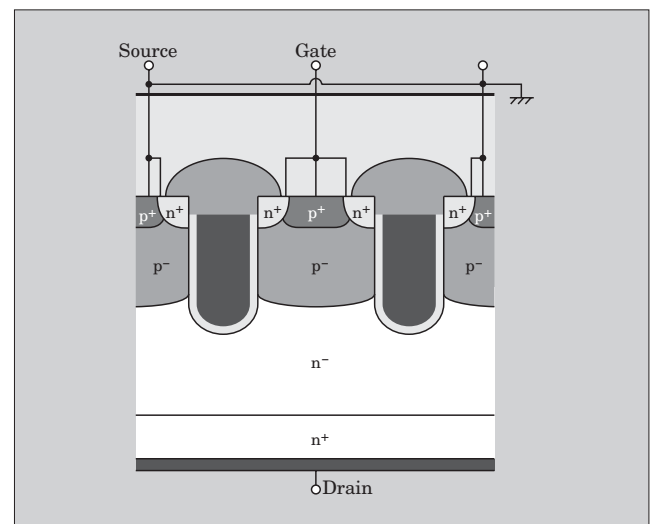
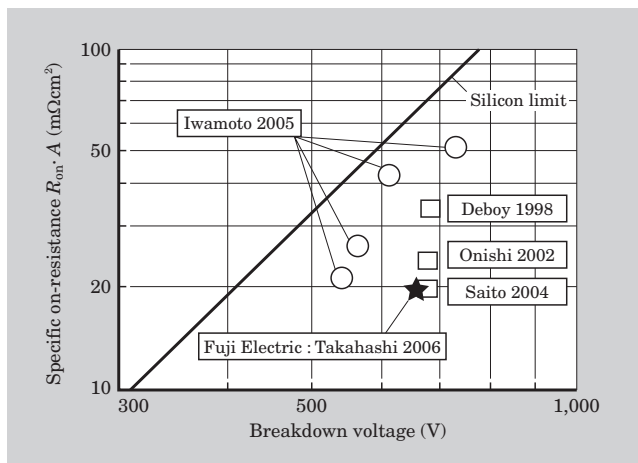


Fig.4 Data presented at scientific conferences concerning the relation between on-resistance and breakdown voltage of high voltage superjunction MOSFETs



and low reverse leakage current (low I_r) SBD series of SBDs and the Super LLD (low loss diode) series of LLDs. Demand for these product groups is extremely strong, and Fuji Electric is working to expand its supply capability.

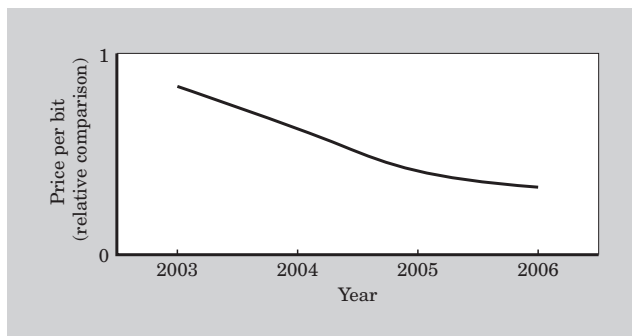
Looking toward the future, Fuji Electric is focusing on research and development aiming for even higher performance and smaller size. An example of Fuji Electric's latest success, shown in Fig. 4, is the attainment of a superjunction MOSFET⁽¹⁰⁾ having the world's highest level of low specific on-resistance of 19.8 mΩcm² (at the breakdown voltage of 660 V) in a prototype of a trench refilled type superjunction MOS FET that is expected to achieve lower cost. This result has been announced at an international conference⁽¹¹⁾.

4. Power ICs

Fuji Electric has achieved many successes with power ICs, including the mass-production of M-Power 2, a power IC for use in high-efficiency low-noise switching-mode power supplies, and the adoption of the M-Power 2 by the major manufacturers of power supplies for LCD (liquid crystal display) TVs, the mass-production of a 4th generation 256-bit PDP (plasma display panel) address driver IC⁽¹²⁾, the development of a 4th generation 96-bit PDP scan driver IC, the mass production of a control IC for quasi-resonant low standby AC-DC switching-mode power supply, the mass production of a multi-channel input integrated power IC for use in an automotive ECU (electronic control unit), the mass-production of a CSP (chip size package)-IPS (intelligent power switch) for use also in the automotive ECU, the development of a control IC for a single-channel DC-DC buck converter, the development of a 2nd generation micro DC-DC converter, and so on.

The M-Power 2 power IC is a 2nd generation product for use in high efficiency and low noise switching-mode power supplies, and the incorporation of Fuji

Fig.5 Trend of decreasing price-per-bit for PDP driver ICs (example of address driver IC)

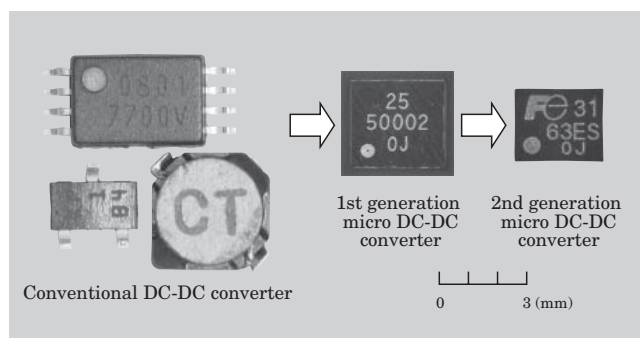


Electric's proprietary control technology enables a current resonant switching-mode power supply without resonant shift to be realized for the first time with a power IC. Because the M-Power 2 enables the easy configuration of high-efficiency low-noise high-power switching-mode power supplies of up to 250 W, its usage is increasing in power supplies for flat panel televisions such as LCDs where noise is undesirable and high efficiency is required. Fuji Electric is also developing the M-Power 2A series which realizes even higher power output with the same package to support larger size flat panel televisions.

PDP driver ICs are power ICs that make full use of Fuji Electric's expert high-voltage technology, and many of Fuji Electric's proprietary technologies have been used in a 100 V BCD (bipolar, complimentary and double-diffused MOS) process for address driver ICs and 200 V SOI (silicon on insulator) process for scan driver ICs. In particular, the 200 V SOI process is the world's first process that integrates IGBTs in a SOI chip⁽¹³⁾, thus enabling a significant reduction in chip area per output bit. Figure 5 shows an example of the decreasing price-per-bit trend for PDP driver ICs. Until now, the price-per-bit for power ICs has been falling steadily due to improved device processes and an increased number of integrated bits per chip. In the future, however, a straight-line decline in prices-per-bit will be difficult to attain due to the unique problem of power ICs of not permitting scaling of the supply voltage, and due to the theoretical limits of silicon material. Fuji Electric intends to provide continuous improvements that benefit the user by introducing LVDS (low voltage differential signal) and RSDS (reduced swing differential signal) technology to reduce the number of signal lines and support electric power recirculation in order to lower the cost and increase the performance of the entire display panel.

In the field of power ICs for switching-mode power supplies and for automobiles, Fuji Electric's strengths are in the high voltage processes that utilize power device technology and in the processes for integrating high voltage devices and high current devices in the ICs. All the processes can integrate 30 V or higher devices, and provide distinctive product groups that

Fig.6 Appearance of 2nd generation micro DC-DC converter

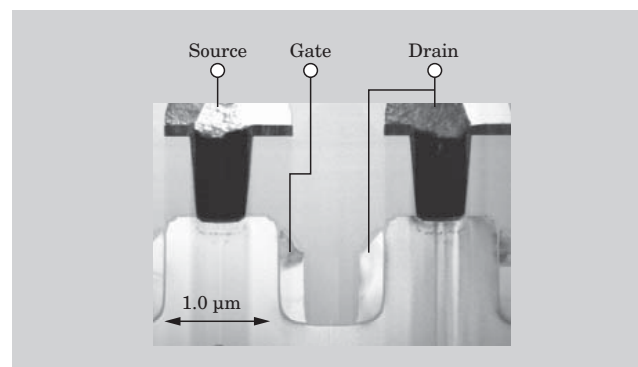


include an integrated 500 V start-up device for use in AC-DC switching-mode power supplies, an integrated 600 V IGBT for use in automotive igniters⁽¹⁴⁾, an integrated 60 V power MOSFET for use in automotive power ICs⁽¹⁵⁾, or integrated 30 V to 60 V low on-resistance DMOS (double diffused MOS) circuits for use in DC-DC power supply ICs and in integrated power ICs for automobiles. Also being used recently is COC (chip on chip) technology which, in addition to these process technologies, involves laminating and integrating into a single package of multiple silicon chips and micro-inductors. COC technology is beginning to demonstrate its effectiveness in achieving smaller sizes and higher outputs. Figure 6 shows the appearance of a 2nd generation micro DC-DC converter, samples of which are presently being deployed. Using COC technology to integrate a micro inductor with a silicon chip already integrated with an output power MOSFET, the world's smallest DC-DC converter was realized with a 1st generation micro DC-DC converter⁽¹⁶⁾. A subsequent 2nd generation micro DC-DC converter achieved an even 40 % smaller size while maintaining the same power output.

To increase the performance and reduce the size of power ICs, it is important that the integrated output power devices provide higher performance and smaller size. For future applications, Fuji Electric is working vigorously to advance its research and development into realizing higher performance and smaller size integrated power devices for power ICs. In particular, such research and development efforts are focusing on Fuji Electric's proprietary three-dimensional TLPM (trench lateral power MOSFET⁽¹⁸⁾) power device for use in Li-ion battery protection ICs⁽¹⁷⁾ and DC-DC converters, and for possible future applications to automobiles. Figure 7 shows a photograph of a cross-section of Fuji Electric's latest device. This device, usable as a high-side switching element, has a $R_{on} \cdot Q_{gd}$ figure of merit of 16.4 mΩnC (at the breakdown voltage of 20 V) and, as a device for integration into a power IC, realizes the world's highest level of performance. This device also attains a high electrostatic discharge withstand capability, which is usually the weak point of this class of devices, of 2 kV with a HBM (human body model)⁽¹⁹⁾.

Fuji Electric is also advancing its research into

Fig.7 Cross section photograph of Fuji Electric's latest TLPM that realizes both the world's highest figure of merit and a high electrostatic discharge withstand capability



digital control⁽²⁰⁾ and is considering the possibility of converting the present analog control to digital control to achieve higher accuracy, lower power consumption and smaller size.

5. Conclusion

Fuji Electric desires to contribute to the development of society and to the protection of the global environment through innovating and popularizing power electronics technology. Power semiconductor devices are one of the key products that support power electronics, and this paper has described the current status and future outlook for the main power semiconductor devices.

For power semiconductor devices to contribute to the development of society and to the protection of the global environment, their transition to higher performance, smaller size, higher reliability and lower cost must be accelerated more than ever. On the other hand, a considerable portion of the relevant technology is thought to be approaching its theoretical limit, and technical innovations are needed in various fields, including materials, processing, device, circuits, packaging, testing and the like. Fuji Electric intends to place extra emphasis on technical development, and to foster a workforce capable of creating new technology and capable of technical innovation

References

- (1) Sluijs, A. et al. Subtropical Arctic Ocean Temperatures during the Palaeocene/Eocene thermal maximum. *nature*. vol.441, 2006, p.610-613.
- (2) Energy Information Administration, U.S. Department of Energy. International Energy Outlook 2004. 2004-04.
- (3) Intergovernmental Panel on Climate Change. Summary for Policymakers. Third Assessment Report. 2001-09.
- (4) Otsuki, M. et al. Investigation on the Short-Circuit Capability of 1200V Trench Gate Field Stop IGBTs. *Proceedings of ISPSD'02*. 2002, p.281-284.
- (5) Otsuki, M. et al. 1200V FS-IGBT Module with Enhanced Dynamic Clamping Capability. *Proceedings of*

- ISPSD'04. 2004, p.339-342.
- (6) Nishimura, Y. et al. All lead free IGBT module with excellent reliability. Proceedings of ISPSD'05. 2005, p.79-82.
 - (7) Onozawa, Y. et al. 1200 V Super Low Loss IGBT Module with Low Noise Characteristics and High dI/dt Controllability. Proceedings of IEEE Industry Applications Conference. Session 10, 2005, p.2.
 - (8) Nishimura, Y. et al. Investigations of all lead free IGBT module structure with low thermal resistance and high reliability. Proceedings of ISPSD'06. 2006, p.249-252.
 - (9) Kobayashi, T. et al. High-Voltage Power MOSFET Reached Almost to the Silicon Limit. Proceedings of ISPSD'01. 2001, p.435-438.
 - (10) Fujihira, T. Theory of Semiconductor Superjunction Devices. Japan Journal of Applied Physics. vol.36, 1997, p.6254-6262.
 - (11) Takahashi, K. et al. $20\text{ m}\Omega\text{cm}^2$ 660 V Super Junction MOSFETs Fabricated by Deep Trench Etching and Epitaxial Growth. Proceedings of ISPSD'06. 2006, p.297-300.
 - (12) Nomiya, T. et al. New 256-ch PDP Address Driver IC with Reducing Switching Noise. Proceedings of IDW/AD'05. 2005, p.453-456.
 - (13) Sumida, H. et al. A High Performance Plasma Display Panel Driver IC Using SOI. Proceedings of ISPSD'98. 1998, p.137-140.
 - (14) Fujihira, T. Smart IGBT for Automotive Ignition Systems. Proceeding of CIPS'00. 2000, p.36-44.
 - (15) Yoshida, Y. A Self-Isolated CDMOS Technology for the Integration of Multi-Channel Surge Protection Circuits. Proceedings of ISPSD'03. 2003, p.101-104.
 - (16) Hayashi, Z. et al. High-efficiency dc-dc converter chip-size module with integrated soft ferrite. IEEE Trans. Magn. vol.39, issue 5, 2003, p.3068-3072.
 - (17) Sawada, M. et al. A Single Chip Li-ion Battery Protection IC Using High Side N-Channel Bi-directional Trench Lateral Power MOSFETs. Proceedings of IPEC-Niigata'05. 2005, p.1386-1393.
 - (18) Fujishima, N. et al. A High-Density Low On-Resistance Trench Lateral Power MOSFET With a Trench Bottom Source Contact. IEEE Transactions on Electron Devices. vol.49, no.8, 2002, p.1462-1468.
 - (19) Matsunaga, S. et al. Low Gate Charge 20 V Class Trench-aligning Lateral Power MOSFET. Proceedings of ISPSD'06. 2006, p.329-332.
 - (20) Trescases, O. et al. A Digitally Controlled DC-DC Converter Module with a Segmented Output Stage for Optimized Efficiency. Proceedings of ISPSD'06. 2006, p.373-376.



IGBT Modules for Electric Hybrid Vehicles

Akira Nishiura
Shin Soyano
Akira Morozumi

1. Introduction

Due to society's increasing requests for measures to curb global warming, and benefiting from the skyrocketing prices of petroleum products, the sales volume of hybrid cars is growing rapidly. By combining the two main types of power sources, gasoline engines and electric motors, and optimizing the load sharing according to the driving conditions, hybrid systems achieve improved fuel economy. These hybrid systems had an extremely high cost when mass-produced cars were first being sold and their sales volume was limited. Subsequently, however, by improving the performance and reducing the cost to car manufacturers, electric equipment manufacturers and component manufacturers, hybrid system costs have fallen and, at present, the sales volume is increasing.

In a gasoline hybrid system, an electric power conversion system that includes an inverter and converter is used to convert the power generated by the engine into electrical energy, to charge and discharge a battery, and to drive the motor. The electric power conversion system typically uses an IGBT (insulated gate bipolar transistor) module as its main switching device. IGBT modules have been used mainly in industrial facilities for the past 20 years, but the development of IGBT modules having higher reliability and higher performance is being advanced for application to automobiles.

This paper introduces the core technologies and examples of product applications relating to the performance and reliability of IGBT modules used in hybrid cars.

2. Reliability Technology for Automotive-use IGBT Modules

2.1 Difference from modules for industrial use

The IGBT module product group used for many years in industrial applications forms the basis for the automotive-use IGBT modules. However, the environment and conditions under which automotive-use products are used are much more severe than those of conventional industrial-use products, and the required

levels of long-term reliability are significantly different. For this reason, automotive-use electric equipment is required to provide long-term reliability, and such equipment often requires two or more years from the start of development until mass production. Efforts to eliminate lead usage are being advanced in order to address environmental issues, but since the desired reliability levels are different for industrial-use⁽¹⁾ and automotive-use IGBT modules, the materials used therein will also differ.

2.2 Requested reliability and compliant technology

An example comparison of the reliability levels required for industrial-use and automotive-use IGBT modules is shown in Table 1. Because automotive-use modules are water-cooled and have a large temperature variation, their required temperature cycle tolerance is an order of magnitude greater than that of the industrial-use modules. If the number of temperature variations (temperature cycles) exceeds the device capability, cracks will appear in the solder layer bonding together the power chips and the insulating substrate and create defects that increase the thermal resistance. Accordingly, the technology that provides the requested level of temperature cycle tolerance must relieve stress at the solder layer. Assuming use in a high temperature and high humidity environment, the migration tolerance of the printed circuit board is also an important issue.

Table 1 Comparison of required levels of guaranteed reliability

Item \ Category	Industrial use	Automotive use
Temperature cycle test	100 cycles Temperature conditions : - 40 to +125°C	1,000 cycles Temperature conditions : - 40 to +125°C
Power cycle test	15,000 cycles Temperature conditions: $\Delta T_j = 100^\circ\text{C}$	30,000 cycles Temperature conditions: $\Delta T_j = 100^\circ\text{C}$
Vibration test	Acceleration = 10 G 2 h for each of X, Y and Z axes	Acceleration = 20 G 2 h for each of X, Y and Z axes

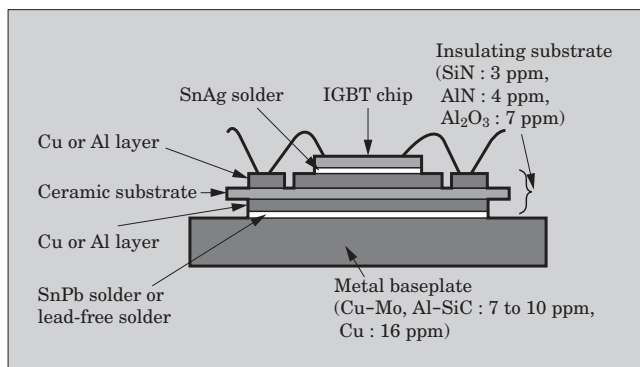
2.3 Reliability technology for lead-free compliance

The automotive industry is addressing environmental issues by working to develop lead-free technology in support of the ELV (end of life vehicles) directive. As described above, however, the high level of required reliability for automotive applications is a restriction that has not resulted in all lead-free automotive electronic components. Figure 1 shows a typical cross-section of an IGBT module. The module is configured bottom-up from a metal baseplate, solder, an insulating substrate (ceramic substrate bonded to metal layers on both sides), solder, an IGBT chip, and bonded wire. Lead-free solder for use underneath the IGBT chip has been developed and is being utilized in industrial-use modules⁽²⁾⁽³⁾.

(1) Solder underneath the insulating substrate

Various trials were carried out on the solder connecting the metal baseplate and insulating substrate in order to solve the problem of cracking caused by the stress of temperature cycles. The metal baseplate and insulating substrate have different rates of thermal expansion, and a change in temperature causes thermal stress to be generated in the solder layer. The elongation of cracks in the solder layer due to this stress is a problem when using lead-free solder. In hybrid vehicle-use IGBT modules, composite materials such as Cu-Mo and Al-SiC that have a small thermal expansion rate (i.e., a thermal expansion rate of 7 to 10 ppm, compared to Cu which has a thermal expansion rate of 16 ppm) have been used previously for the metal baseplate, and this is one way to prevent the abovementioned problem. However, the problems with these materials are that their thermal conductivities (indicating exothermicity), in the range of 150 to 250 W/m·K, are lower than that of copper (Cu having a thermal conductivity of 390 W/m·K), and their cost is several times that of copper. Figure 2 shows an example of a thermal stress simulation (with a 1/4 model) performed for the purpose of using copper, which has a relatively low cost and good exothermicity, as the baseplate material. Also, Fig. 3 shows the results of temperature cycle testing using a sample in which the solder material was changed.

Fig.1 Cross section of IGBT module



From Fig. 2, the deformation and stress in the given model can be inferred. In Fig. 3, the actual state of an elongating crack, according to the solder composition, can be verified. This type of three-dimensional analysis was carried out in detail, and by comparing the analysis results to actual experimental results, we found that a structure using a copper baseplate and lead-free solder would be able to provide the required level of reliability for automobile applications.

(2) Improved reliability of printed circuit boards

Since the reflow temperature increases when lead-free solder is used to mount electronic components, care must be taken when using the conventional FR-4 circuit board which has low heat-resistance. The migration and temperature cycle tolerances required of automotive-use devices are gradually becoming more severe. The use of higher heat-resistance and halogen-free low thermal expansion rate circuit boards enable improvement in both the migration tolerance and the temperature cycle tolerance. Figure 4 shows the change in insulation resistance during high temperature high humidity bias testing in which a voltage of 1,200 V is applied to a pattern having a narrow spacing of 0.5 mm. It can be seen that this halogen-free substrate has excellent capability to withstand 2,000 hours or more of testing.

Fig.2 Thermal stress simulation of IGBT module (1/4 model)

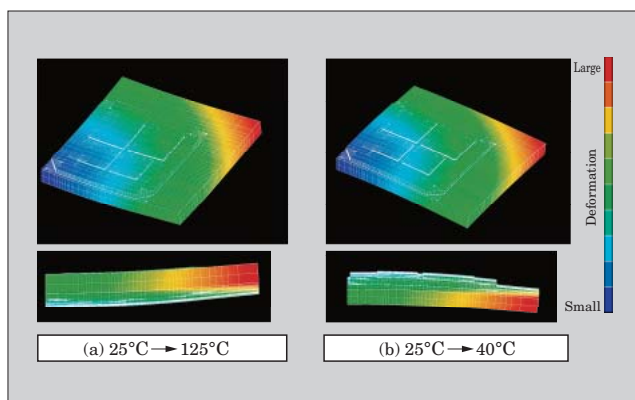
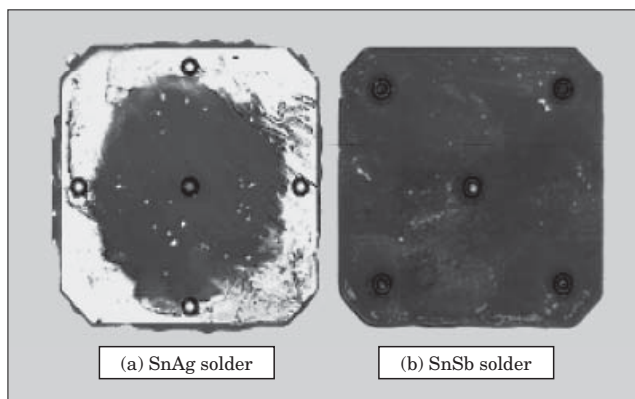


Fig.3 Ultrasound photograph focused underneath the substrate after 2,000 cycles of a temperature cycle test (The white area is the solder crack.)



IGBT modules are high voltage devices, and high voltage lines lay side-by-side on the printed circuit board connected to the module. To ensure safety, ion-migration on the substrate surface must not degrade electric strength, and the resulting large margin of safety provides a sense of security.

(3) Lead-free solder for through-holes

IGBT modules are used in combination with a drive circuit and protection circuit, and therefore, the solder technology for connecting the printed substrate to the module is extremely important. Moreover, since in an IPM (intelligent power module), a printed circuit board is attached inside the module package, the lead-free solder used is required to be capable of withstanding the same number of temperature cycles as the IGBT module. The use of lead-free solder is also required at the location of the through-hole connecting the printed circuit board and the module, and lead-free solder has been developed for this purpose. Figure 5 shows a cross section after temperature cycle testing of a through-hole joint structure in which SnAg lead-free solder having improved durability was used. Due to the low rate of thermal expansion in the thickness direction of approximately one-half that of the FR-4, cracking is limited even after 2,000 cycles, and the required level of durability is achieved.

Fig.4 Change in insulation resistance during high temperature high humidity bias test

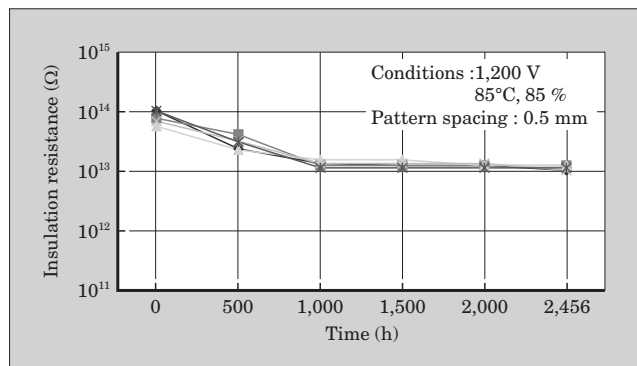
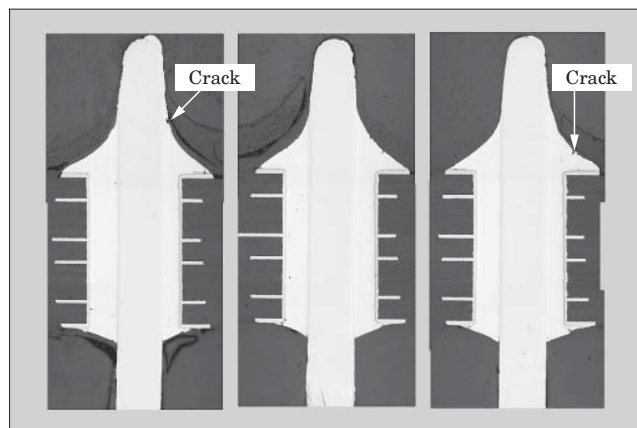


Fig.5 Cross section of through hole joint (after 2,000 temperature cycles)



3. IGBT-IPM for Electric Hybrid Vehicles

An overview of the hybrid vehicle-use IGBT-IPM, as developed based on the above-described core technologies for IGBT modules, is presented below. Figure 6 shows views of the exterior and interior of the hybrid vehicle-use IGBT-IPM.

3.1 IPM overview

The IPM is a switching device rated at 600 A and 1,200 V for use in an up/down converter, and is configured from an upper arm and a lower arm. Each arm is provided with four IGBT chips and four FWD (free wheeling diode) chips connected in parallel configuration, gate drive circuits, protection circuits, chip temperature output circuits are also provided on the printed circuit board inside the IPM.

3.2 Composition of packaging

Since copper is used for the metal baseplate, the difference in thermal expansion rate compared to the insulating substrate causes bending stress to be generated. The use of an insulating substrate made of aluminum oxide, a high-strength ceramic able to resist bending stress, makes it possible to use a copper baseplate. SnSb is used as the lead-free solder underneath the insulating substrate in order to strengthen the resistance to cracking. Since the solder layer stress caused by bending stress is largest in the area around the insulating substrate, the shape of that area is designed to resist solder cracking.

The aluminum wires that electrically connect the power chip have a diameter of 400 μm, which provides excellent power cycle performance, and ensures a strong connection with low resistance. A halogen-free circuit board with improved heat-resistance is used as the printed circuit board, thereby ensuring sufficient temperature cycle tolerance and migration tolerance.

3.3 U series IGBT chip and FWD chip

Fuji Electric's 1,200 V U series chips, having a good market performance in industrial applications, are being used as the IGBT chip and FWD chip in the

Fig.6 Hybrid vehicle-use IGBT-IPM

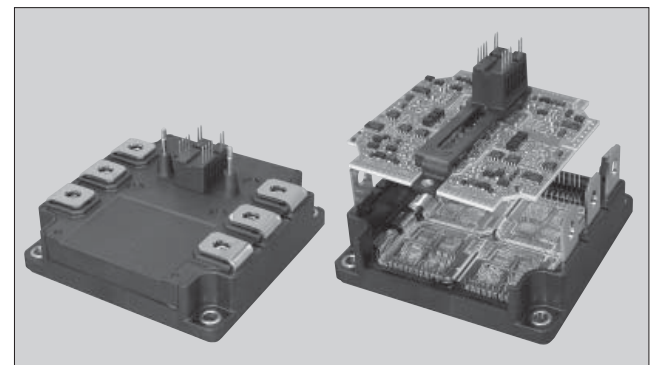
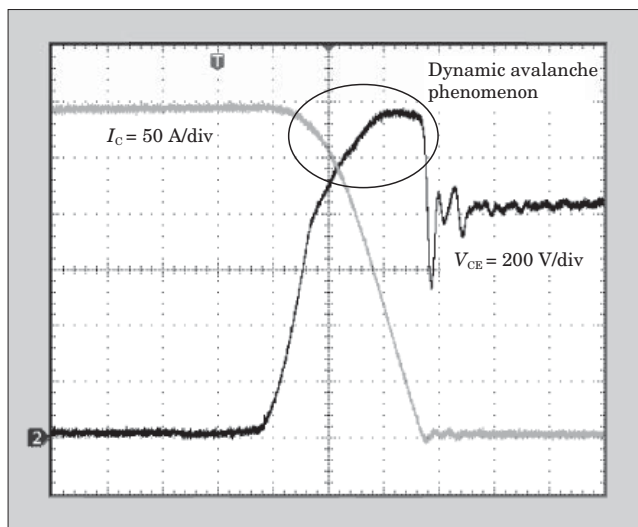


Fig.7 Dynamic avalanche waveform of U series IGBT chip



IGBT-IPM. The U series IGBT chip is a trench gate type chip, corresponding to a 5th generation IGBT, and has characteristics of both a low $V_{CE(sat)}$ and high tolerance of dynamic avalanching. Figure 7 shows the dynamic avalanche waveform of the U series IGBT chip. The dynamic avalanche phenomenon absorbs the surge voltage energy emitted at the time when a large current turns off. The U series FWD has a low injection efficiency type anode structure and higher transfer efficiency. V_F characteristic has a positive temperature dependence and low variation.

3.4 Protective functions

All IGBTs are provided with overcurrent protection and overheating protection functions to prevent damage to the IGBT. Moreover, as a special function for automotive-use IGBTs, a function that externally outputs

as an analog signal of the IGBT chip temperature in each of the upper and lower arms is provided to enable monitoring from an operating situation.

4. Conclusion

The core technologies that make possible the realization of highly reliable and lead-free IGBT modules for hybrid vehicle use and Fuji Electric's product line have been introduced. The sales volume of hybrid vehicles will continue to increase and IGBT modules will continue to be used for electric power conversion for the foreseeable future. Accordingly, manufacturers who have not previously produced such modules are expected to enter this market, and the competition to develop new technology is expected to intensify. In the future, Fuji Electric intends to continue to develop modules that provide even higher reliability, smaller size and higher heat dissipation, and that are easier to use.

References

- (1) Nishimura, Y. et al. Investigations of all lead free IGBT module structure with low thermal resistance and high reliability. Proceedings of the 18th International Symposium on Power Semiconductor Devices & ICs. 2006, p.285-288.
- (2) Morozumi, A. et al. Reliability of Power Cycling for IGBT Power Semiconductor Modules. IEEE Transactions on Industry Applications. Vol.39, No. 3, May/June 2003, p.665-671.
- (3) Nishimura, Y. et al. All lead free IGBT module with excellent reliability. Proceedings of the 17th International Symposium on Power Semiconductor Devices & ICs. 2005, p.79-82.

New Concept IGBT-PIM Using Advanced Technologies

Yasuyuki Kobayashi
Rikihiro Maruyama
Eiji Mochizuki

1. Introduction

With the dramatic development of power electronics in recent years, IGBT (insulated gate bipolar transistor) modules have become the mainstream semiconductor devices used in industrial power conversion applications, and are being applied in a wide range of fields including manufacturing, transportation, home electronics and the like. With each successive generation, IGBT modules have incorporated novel technology to realize energy savings, higher efficiency, smaller size, lower cost and higher reliability. Also, in order to realize higher integration to comply with requests for smaller size and higher performance inverters, IGBT modules have developed into PIMs (power integrated modules), in which an inverter circuit, an input rectifier circuit and a dynamic braking circuit for regeneration are all housed within a single package. Fuji Electric has previously brought to market a 3rd generation N series PIM in 1995, a 4th generation S series Econo-PIM in 1999, and a 5th generation U series in 2002. Requests for smaller size and lower cost machines have been especially strong in recent years, and in response to such requests Fuji Electric has newly developed IGBT-PIMs that incorporate the latest chip package technology. This paper introduces Fuji Electric's latest IGBT-PIM technologies and product lineup.

2. Challenges in Achieving Smaller Size and Higher Integration

Shrinking the die size is an extremely effective technique for realizing the smaller size and lower cost required by the market in recent years. However, shrinking the die size causes an increase in thermal resistance $R_{th(j-c)}$ and also a simultaneous rise in chip temperature as expressed by Equation (1) (where ΔT_{j-c} is the width of the temperature rise), and therefore lower power dissipation and higher heat dissipation of the chip are requirements.

$$\Delta T_{j-c} = \text{power dissipation} \times R_{th(j-c)} \dots\dots\dots (1)$$

In order to reduce power dissipation, not only must the on-state voltage be reduced, but higher speed switching must also be adopted to reduce switching

loss. However, noise radiation will increase as a result. The level of noise radiation is limited by the European standard EN61800-3 and the like. Overcoming this tradeoff between lower power dissipation and noise radiation has presented a new challenge in recent years. As a solution, in 2005 Fuji Electric fully incorporated the latest chip technologies to develop the U4 series of chips in which the noise and power dissipation characteristics were optimized. Also, due to the smaller size and higher density mounting of these chips, it is necessary to develop a package having higher heat dissipation capability, and it is also necessary to increase the mounting efficiency by adopting a high heat dissipating DCB (direct copper bonding) substrate (insulating ceramic substrate), to eliminate thermal coupling, and to use an optimized internal layout, etc. Additionally, RoHS*1 compliance is also a recent requirement of the marketplace. Accordingly, products must be developed so as to satisfy all of these challenges.

3. Characteristics of New Concept IGBT-PIMs

Product development based on the following concepts was carried out to realize not only energy savings, higher efficiency and higher reliability, but also smaller size, higher integration, and lower cost.

- (1) Coexistence of low noise and low power dissipation
 - Improved tradeoff between noise and power dissipation through applying IGBT chips that utilize the latest technology and FWD (free wheeling diode) chips
 - Lower noise realized through improved internal layout of package
 - (2) Realization of small package size and low cost
 - Use of a high heat dissipating new DCB substrate
 - Optimal chip layout to eliminate thermal coupling
 - Optimal internal layout to increase chip mounting efficiency
- Adopting the above concepts, the die size was re-

*1: RoHS is restriction of the use of certain hazardous substances in electrical and electronic equipment.

duced by approximately 30 % compared to the conventional die size, and higher integration was realized.

- (3) Realization of 1,200 V/150 A PIM in conventional EP3-size package

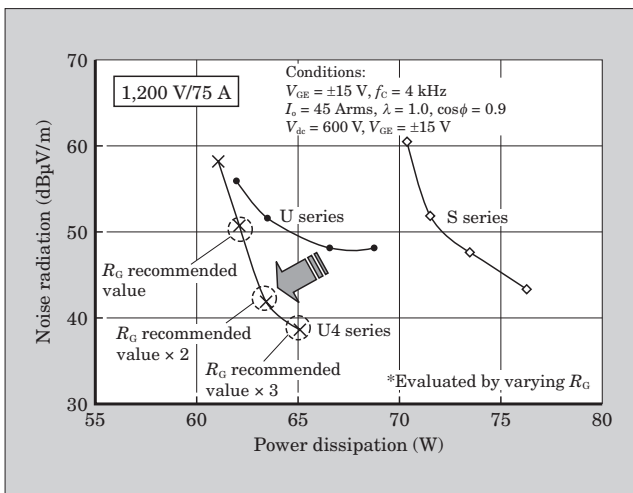
4. Latest Chip Technology

The 1,200 V/1,700 V U series of IGBTs developed in 2002 are the latest models of Fuji Electric's IGBT chips that utilize a trench gate structure and a field stop (FS) structure⁽¹⁾. Further improving the characteristics of this technology, Fuji Electric has also developed an easy-to-use 1,200 V/1,700 V U4 series of IGBT modules (U4-IGBT). Specifically, optimization of the trench gate structure enabled the turn-on speed controllability to be improved compared to a conventional trench IGBT, and the decrease in Miller capacitance (C_{res}) enabled an approximate 30 % reduction in turn-on loss. The noise radiation during switching depends not only on the reverse recovery characteristics of the FWD, but also on the IGBT turn-on characteristics which determine the reverse recovery characteristics of the FWD. Therefore, to reduce noise radiation, both the FWD and the IGBT characteristics must be optimized.

It has been reported that oscillation from a resonant closed loop circuit between the IGBT module and snubber capacitance constitutes a radiation source and is the mechanism by which noise radiation is generated, and that di/dt and dv/dt during switching trigger the resonance. In particular, the resonance condition is determined by di/dt and dv/dt when the IGBT is turned on, and the reverse recovery characteristics of the FWD are similarly determined by the turn-on characteristics.

The U4-IGBT enhances the above-described chip characteristics to realize improved di/dt and dv/dt controllability at turn-on and reduced turn-on loss, and improved tradeoff between noise radiation and power dissipation as shown in Fig. 1.

Fig.1 Tradeoff between noise radiation and power dissipation



5. Latest Package Technology

5.1 Optimal internal pattern layout

(1) Eliminating thermal coupling

In an IGBT-PIM containing multiple power chips within the same package, since all elemental devices emit heat during actual inverter operation, heat becomes concentrated within the package interior due to thermal coupling among neighboring chips. In order to realize the smaller product sizes required in the marketplace, the concentration of heat due to thermal coupling must be eliminated. Therefore, when developing the new package, we used three-dimensional FEM (finite element method) thermal analysis to investigate and optimize the internal chip layout. Figure 2 compares the temperature distributions in conventional and new packages, for the same package size. In the conventional package, power chips are concentrated in the vicinity of the package center, and therefore the chip temperature at the center of the package is higher due to the effect of thermal coupling. On the other hand, in order to eliminate thermal coupling among power chips, the chip layout and chip spacing were optimized in the new package. As the result, the temperature distribution became nearly uniform, and the effect of decreasing T_j by a maximum of 10°C was verified.

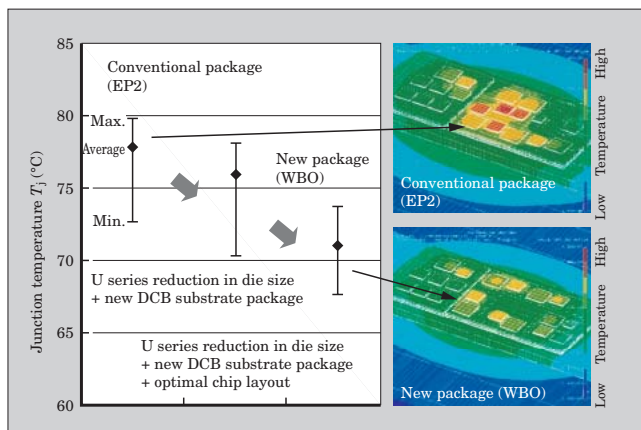
(2) Improving the chip mounting efficiency

With a thermally distributed chip layout and optimal DCB pattern layout, the new package increases the chip installation area ratio from 16.7 % to 26.1 % and increases the chip mounting efficiency by 56 %.

5.2 Technology for reducing noise

An inverter must be designed so that the noise radiation in the frequency range of 30 MHz to 1 GHz is at a level that conforms to certain standards. It has been reported that oscillation from a resonant closed loop circuit between the IGBT module and snubber circuit constitutes a radiation source and is the mechanism

Fig.2 Comparison of temperature distributions according to FEM thermal analysis



by which noise radiation is generated in this frequency region. Maxwell's equation for a distant field is expressed as:

$$E = 1.32 \times 10^{-14} \times f^2 \times S \times I/r \dots\dots\dots (2)$$

(where f is frequency, I is current, S is current loop area, and r is distance),

and a distant field is also dependent on the current closed loop area of the snubber circuit and switching element. Accordingly, in order to reduce the P-N current loop area inside the package, we improved the DCB copper pattern wiring, and tested and studied not only element characteristics, but also the package itself for the purpose of reducing noise. As a result, as shown in Fig. 3, the P-N current loop area was decreased by approximately 50 % compared to a conventional package, and as shown in Fig. 4, the peak value of noise radiation was decreased by approximately 5 dB. Consequently, the turn-on speed can be increased further, and a reduction in switching loss is anticipated.

5.3 Development of new DCB substrate

Figure 5 shows cross sections of IGBT modules (including PIMs). The heat generated by the IGBT chip and FWD chip is conducted through the DCB substrate and copper base plate, and dissipated by the cooling fin. Compared to other materials, the thermal properties of highly strong but less expensive alumina ceramic material are inferior. The thermal conductance of the copper in the DCB substrate is 390 W/m·K, and the alumina ceramic for an insulating layer typically has a thermal conductance of 20 W/m·K, with the ceramic

material acting as a heat insulating barrier. In order to lower the thermal resistance of the DCB substrate, the ceramic material was formed into a thin plate and its thermal conductance improved. On the other hand, based on the results of recent development work, it is understood that reducing the heat flux (heat concentration) per unit area is an effective way to improve the heat dissipation capability. While developing this product, in order to realize lower cost and higher reliability, we considered using alumina ceramic material for the base, as had been done in the past. However, eventually, we adopted the following specific strategy and developed the new DCB substrate⁽²⁾.

- (1) Use a ceramic having high thermal conductivity to ensure long-term reliability and mechanical strength (conductivity: 28 W/m·K)
- (2) Increase the thickness of the DCB substrate copper foil from the existing thickness of 0.25 mm to 0.6 mm in order to disperse heat and reduce the heat flow per unit area
- (3) Achieve higher reliability by increasing the copper foil thickness to remove the constraint on the coefficient of linear expansion that had been imposed by the conventional ceramic material

Figure 6 shows the results of thermal resistance evaluated by the ΔV_{CE} method. We verified that products using the new DCB substrate had lower thermal resistance $R_{th(j-c)}$ by approximately 25 to 30 % than

Fig.3 Internal layout for lower noise

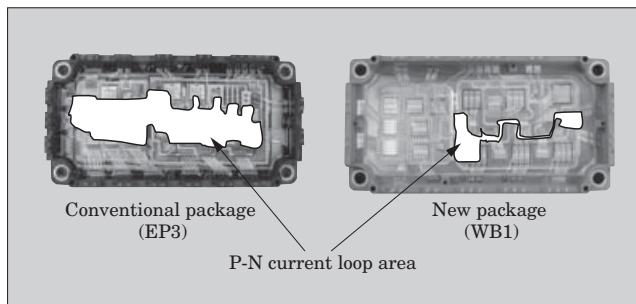


Fig.4 Comparison of noise radiation

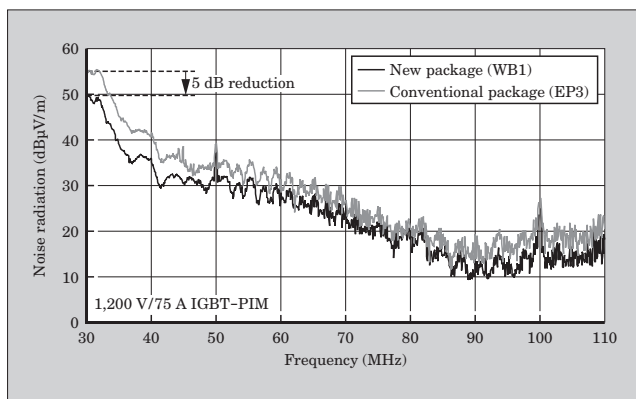


Fig.5 Cross section comparison of IGBT modules

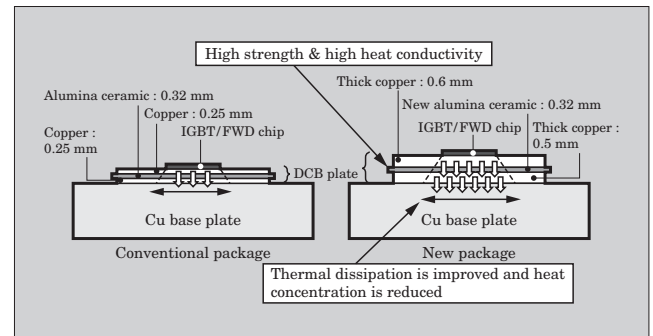


Fig.6 Comparison of transient thermal resistance characteristics

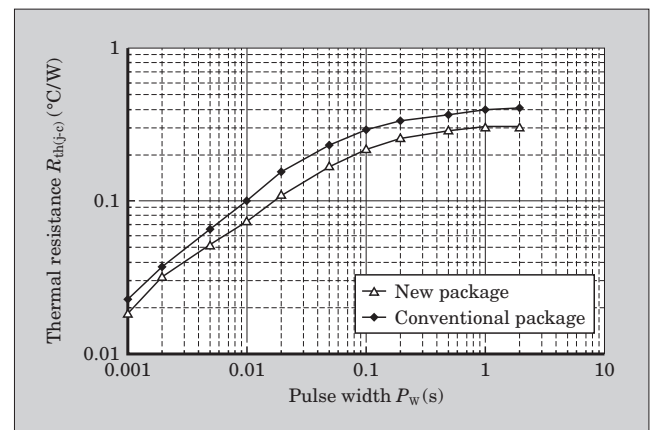


Table 1 Lineup of IGBT-PIM products using next generation package

Break-down voltage	Rated I_c (A)	15	25	35	50	75	100	150
1,200 V	Existing package U/U4 series	M711 (EP2) 107.5×45 (mm)						
				M712 (EP3) 122×62 (mm)				
	New package U4 series							
		M719 (WB0) 107.5×45 (mm)			M720 (WB1) 122×62 (mm)			
Break-down voltage	Rated I_c (A)	15	25	35	50	75	100	150
600 V	Existing package U2 series	M711 (EP2) 107.5×45 (mm)				M712 (EP3) 122×62 (mm)		
	New package U2 series							
					M719 (WB0) 107.5×45 (mm)		M720 (WB1) 122×62 (mm)	

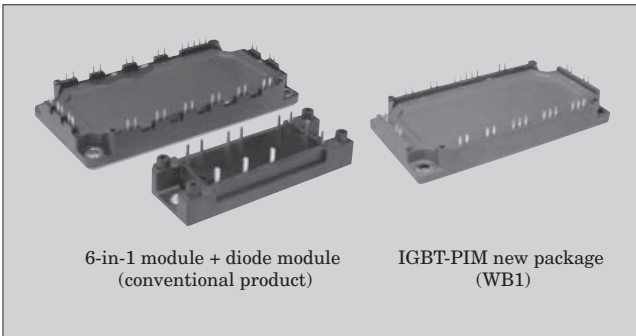
products using the conventional DCB substrate.

This new DCB substrate is selectable as well as AlN and SiN substrates which have high thermal conductance.

6. New Product Lineup

Combining the above-described latest chip technologies with newly developed package technology, Fuji Electric has developed the world's first ultra-small IGBT-PIM, and the 1,200 V series of these devices realizes a current rating that is twice as large as that of conventional device in a package of the same size. Table 1 shows Fuji Electric's lineup of packages for the newly developed IGBT-PIM, and Fig. 7 compares the exterior views of 1,200 V/150 A packages. This lineup

Fig.7 Comparison of external appearances of 1,200 V/150 A conventional and new package products



of new products is expected to enable equipment to be made with smaller size and lower cost. Also, these products were designed in consideration of environmental issues, and this product lineup complies with the RoHS directive, a recent environmental regulation.

7. Conclusion

As IGBT modules have progressed toward lower loss in recent years, the issue of noise radiation has once again become a concern. This paper has introduced new products from Fuji Electric that combine the latest chip and package technologies for the main purposes of reducing noise and size and lowering cost.

Fuji Electric will continue to endeavor to realize elemental devices having higher levels of performance and reliability, to raise the level of its technology in order to resolve new issues and support new marketplace needs, and to contribute to the development of power electronics.

References

- (1) Laska, T. et al. The Field Stop IGBT (FS IGBT) A New Power Device Concept with a Great Improvement Potential. Proc. 12th ISPSD '00. 2000. p.355-358.
- (2) Nishimura, Y. et al. New generation metal base free IGBT module structure with low thermal resistance. Proc. 16th. ISPSD '04. 2004. p.347-350.

All Lead-free IGBT Modules and IPMs

Yoshitaka Nishimura
Tatsuo Nishizawa
Eiji Mochizuki

1. Introduction

It has been reported that acid rain caused by changes in the global environment is causing lead to be discharged from the solder in discarded electrical devices, and that this lead ends up polluting groundwater. As a result, lead-free solder is being used more and more (in compliance with the European Union's RoHS directive*1) instead of the conventional SnPb solder for mounting electronic components. Accordingly, it is desired that IGBT (insulated gate bipolar transistor) modules and IPMs (intelligent power modules) also are made "all lead-free."

In April 2005, Fuji Electric began supplying highly-reliable RoHS-compliant (all lead-free) IGBT modules. As a result, Fuji Electric's annual quantity of lead usage in IGBT modules decreased by approximately 1.5 tons in the 2005 fiscal year, and an additional decrease of 1 ton is anticipated for the 2006.

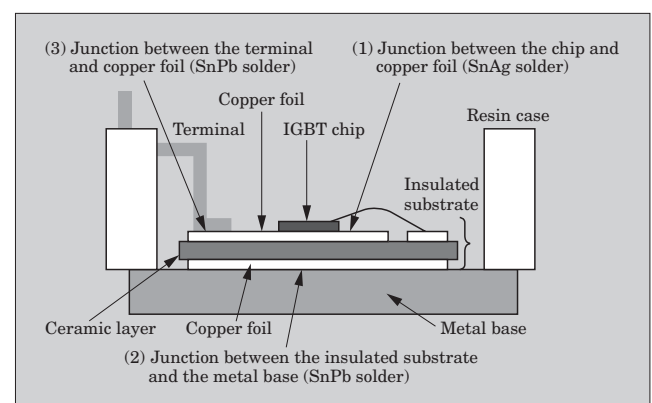
This paper introduces Fuji Electric's all lead-free compliant technology and product line of RoHS-compliant IGBT modules and IPMs.

2. Locations that can be made Lead-free in IGBT Modules and IPMs

Lead used in IGBT modules and IPMs is mainly contained in the solder material. The use of lead-free solder involves the challenges of: (1) ensuring sufficient reliability as a result of the change in solder material, and (2) higher mounting temperatures when using lead-free solder. The challenge of higher mounting temperature can be overcome by changing the materials used to increase the thermal resistance and by changing the mounting devices.

The structure of Fuji Electric's IGBT modules and IPMs is shown in the schematic diagram of Fig. 1. Solder material is used in three locations: (1) the junction between the chip and copper foil, (2) the junction between the insulated substrate and the metal base, and (3) the junction between the terminal and copper

Fig.1 Structure of conventional Fuji Electric IGBT module and IPM



foil. Lead-free solder has been used in location (1) since 1998, and the ability to withstand power cycles of this lead-free solder has been successfully improved. Therefore, our new development aimed to make locations (2) and (3) lead free.

3. Making the Junction between the Insulated Substrate and Metal Base Lead-free

We selected and considered typical SnAg solder and SnAgIn solder for use in a lead-free junction between the insulated substrate and metal base.

(1) Thermal cycling tests

Figure 2 shows the results of thermal cycling tests when various types of solder are used. When using typical SnAg solder, cracking occurred over approximately 30 % of the soldered area after 300 cycles in the thermal cycle test. When using the newly developed SnAgIn solder, however, almost no cracking occurred and the reliability was nearly the same as that of conventional lead solder.

The mechanism that improves the reliability of products using SnAgIn solder was compared to SnAg solder and verified by observing the microstructure of the fractured section and by performing a FEM (finite element method) analysis.

Figure 3 shows the results of an analysis of the stress-strain distribution generated by solder material

*1: RoHS is restriction of the use of certain hazardous substances in electrical and electronic equipment.

Fig.2 Results of ultrasonic monitoring of thermal cycling test

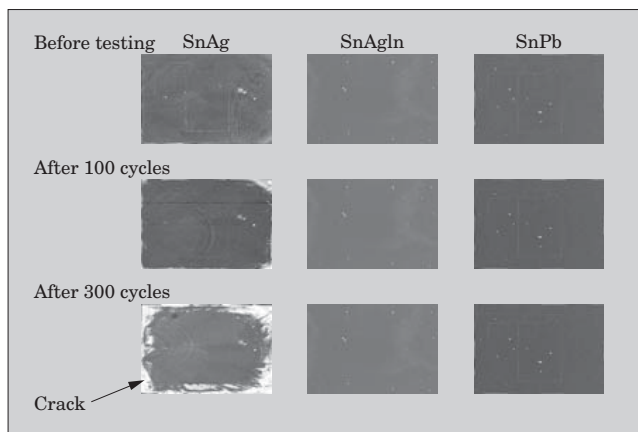
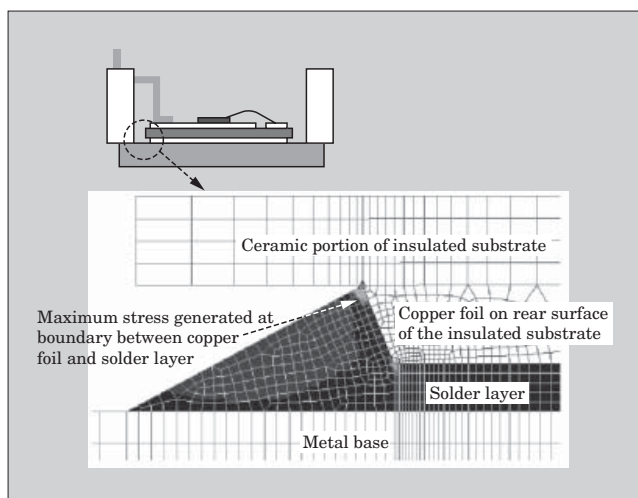


Fig.3 Results of simulated thermal stress of solder between insulated substrate and metal base (FEM analysis results)



underneath the IGBT module during a thermal cycle test. In this drawing, the maximum stress is generated near the boundary between copper foil on the rear surface of the insulated substrate and the solder layer.

Figure 4 shows the results of the fractured solder surface observed using a SEM (scanning electron microscope) after thermal cycle testing. The SnAg solder material was fractured at the boundary between SnAg and CuSn alloys in the vicinity of the copper foil on the rear surface of the insulated substrate. On the other hand, SnAgIn solder fractures not at the boundary between the CuSn alloy layer and the SnAgIn solder, but at the SnAgIn bulk solder layer, and the difference in fractured states can be seen clearly.

(2) Tensile strength test

Figure 5 shows the results of tensile strength tests of bulk SnAg and bulk SnAgIn solder material. Bulk SnAgIn solder material has a strength of approximately 1.5 times than that of SnAg solder. SnAg solder is observed to have coarser particles as the thermal cycling test progresses. Strength typically decreases as particles become coarser.

Fig.4 SEM view of fractured area of SnAg and SnAgIn solder after thermal cycling test

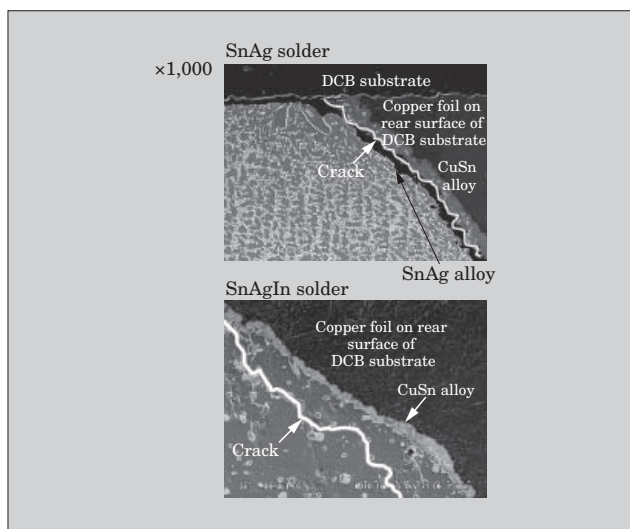
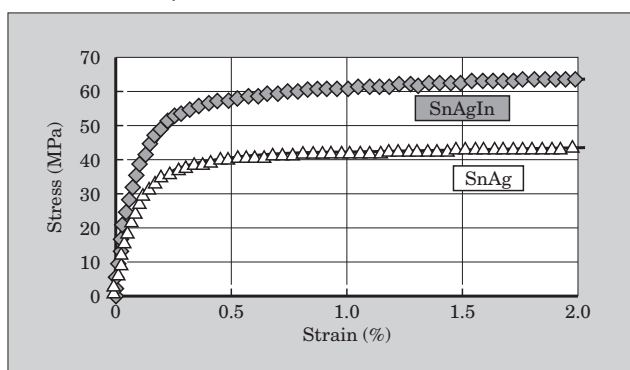


Fig.5 Results of tensile test for SnAg and SnAgIn solder at room temperature



Based on the above results, the addition of In to the SnAgIn solder results in: ① suppression of the formation of a SnAg alloy layer, resulting in a change from fracturing at the alloy boundary to fracturing of the bulk solder material, ② an approximate 1.5 times improvement in bulk strength, and ③ particles that do not become coarser during thermal cycling tests. These factors are thought to improve the ability to withstand the thermal cycling tests.

4. Making the Junction between the Terminal and Insulated Substrate Lead-free

We compared and considered SnAg solder and conventional SnPb solder for use in a lead-free junction between the terminal and insulated substrate.

(1) Thermal cycling tests

The results of observation of the fractured section of solder material obtained after 300 cycles in a thermal cycling test showed no cracks in either SnAg solder or SnPb solder. From these results, we computed the stress and strain generated in the terminal area during the thermal cycling test, and speculated the

reason that the thermal cycling test lifespan is longer for typical SnAg solder. Figure 6 shows the computed results. In contrast to the previously described junction between the insulated substrate and the metal base, it can be seen that the maximum strain is generated in a bulk solder area at the junction between the terminal and the insulated substrate. Because maximum strain is generated in the bulk solder material, the thermal fatigue lifespan of the terminal area solder can be estimated using the Coffin-Manson law for bulk solder material.

(2) Fatigue life testing

In order to assess the number of cycles to failure for bulk solder material, we implemented isothermal fatigue life testing of bulk solder material. The fatigue tests of the bulk materials were performed under the conditions of 25°C room temperature, 0.02 %/s strain rate. The life span was determined to be the number of cycles when the applied stress was reduced 25 %. Figure 7 shows the results of the fatigue life testing. The graph shows the number of cycles to failure (fatigue life) for each type of solder when stress is reduced by 25 % from the initial stress within the inelastic strain range. The amount of strain generated at the soldered portion of the terminal as estimated from the

Fig.6 Distribution of stress at junction between terminal and DCB substrate

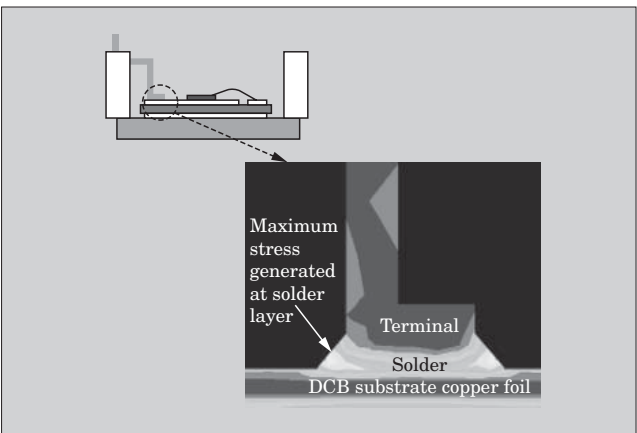
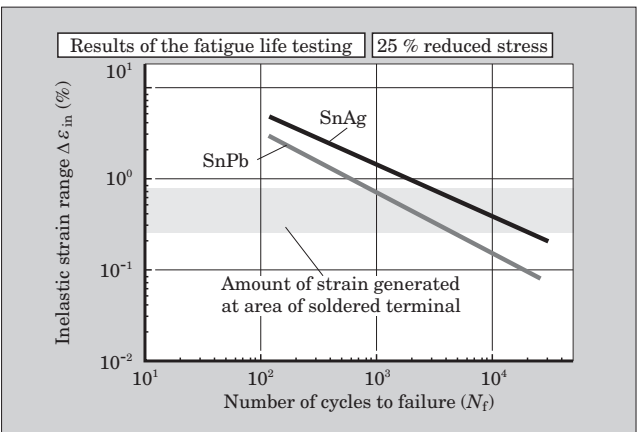


Fig.7 Coffin-Manson plots for SnAg alloy and SnPb alloy



results of Fig. 6 is also shown. For withstanding generated strain, it can be seen that SnAg solder has the same or longer lifespan than SnPb solder.

Based on the Coffin-Manson plots of Fig. 7, it is thought that SnAg solder, used in the junction between the terminal and the insulated substrate in an IGBT module or IPM structure, will exhibit the same or longer lifespan as SnPb solder. This result is consistent with the results of thermal cycle testing of the terminal area of actual devices.

Based on the above results, we selected SnAg solder as a lead-free solder material for use in the junction between the terminal and the insulated substrate, and have realized the same or higher reliability as with conventional products.

5. RoHS-compliant IGBT Module and IPM Series

Fuji Electric's RoHS-compliant IGBT module and IPM series are listed in Table 1 and examples of the

Table 1 Fuji Electric's RoHS-compliant IGBT product line

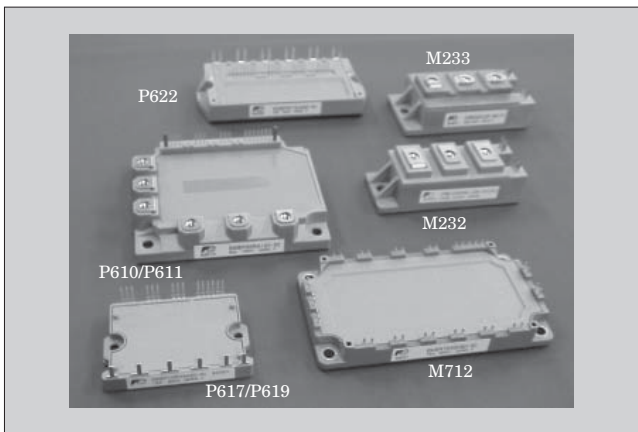
(a) IGBT module

	10 A	15 A	20 A	25 A	30 A	50 A	75 A	100 A	150 A	200 A	225 A	300 A	400 A	450 A
600 V	M711 (EP2)						M712 (EP3)							
							M633							
	M717 (Small Pack)						M636		M232		M233			
1,200 V	M711 (EP2)						M712 (EP3)		M254					
							M636		M633					
							M232							
	M717 (Small Pack)										M233			
													M235	

(b) IPM

	10 A	15 A	20 A	25 A	30 A	50 A	75 A	100 A	150 A	200 A	225 A	300 A	400 A	450 A
600 V	P617/P619					P610/P611								
						P622 (Econo-IPM)								
1,200 V			P610, P611											
	P619		P622 (Econo-IPM)											

Fig.8 Example of Fuji Electric's RoHS-compliant IGBT modules and IPM packages



product packages are shown in Fig. 8. Fuji Electric is expanding its lineup of RoHS-compliant products sequentially, beginning with low-end devices used in consumer products which are easily discarded.

6. Conclusion

Fuji Electric's RoHS-compliant technology and product lineup of IGBT modules and IPMs have been introduced. These products are environmentally friendly and achieve the same or higher level of reliability as present-day lead solder products.

Through using this technology to develop all lead-

free IGBT module and IPM products, Fuji Electric aims to help protecting the global environment.

References

- (1) Morozumi, A. et al. Reliability of Power Cycling for IGBT Power Semiconductor Modules. IEEE Transactions On Industry Applications. Vol. 39, no. 3, 2003-05/06, p. 665-671.
- (2) Nishimura, Y. et al. All lead free IGBT module with excellent reliability. Proceedings of the 17 International Symposium on Power Semiconductor Devices & ICs. May 23 – 26, 2005, Santa Barbara, CA.



Development of Pressure Sensor Cell for Fuel Leak Detection

Katsuyuki Uematsu
Shigeru Shinoda
Shojiro Kurimata

1. Introduction

As a result of the OBD (on-board diagnostic system) regulations in the US market, gasoline evaporative leak detection for fuel tank systems is increasingly being required. Highly sensitive pressure sensors that can measure a 10 kPa range of relative pressure are utilized to detect gasoline evaporative leakage.

Fuji Electric has developed a pressure sensor cell for fuel leak detection (FTPS: fuel tank pressure sensor) that uses a CMOS process-based digital trimming scheme. This paper presents a product overview, discusses considerations relating to the high sensitivity and burst pressure design, and reports the results of a product evaluation.

2. Features

Figure 1 is an overview of the pressure sensor cell for fuel leak detection (FTPS). A conventional pressure sensor has two chips, one is a sensor gauge and the other is an analog circuit to compensate the sensor characteristics and amplify the output signals from the sensor gauge. Furthermore a conventional pressure sensor also needs EMC (electromagnetic compatibility) protection devices such as chip capacitors, chip resistors or SMD (surface mounted device) filters. Therefore the conventional pressure sensor may have increased susceptibility to failure due to many soldered

and wired electric connections between the terminals of chips and other components.

Fuji Electric has developed the FTPS using integrated single-chip technology to achieve a downsized and highly reliable pressure sensor.

Concepts of the FTPS development are listed below.

- (1) "All in one chip" configuration including a sensor gauge, amplifier, compensation circuit, noise and surge protection devices, and diagnostic circuit all integrated into a single chip
- (2) Downsizing by using Fuji Electric's standard small pressure sensor cell package
- (3) World's smallest one-chip pressure sensor with installed EMC compliant
- (4) Reduced cost through production with Fuji Electric's common facilities for producing standard pressure sensor cell packages
- (5) High sensitivity and high burst pressure by using Fuji Electric's proprietary diaphragm etching process

3. Structure of the FTPS

Figure 2 shows an overview and cross section of the sensor unit for the FTPS. A Wheatstone bridge configured from four diffused piezo resistors is on the diaphragm. To achieve high sensitivity and high burst pressure, the diaphragm is etched by Fuji's proprietary isotropic etching process to form a round shape.

The output voltage of the Wheatstone bridge is am-

Fig.1 FTPS cell

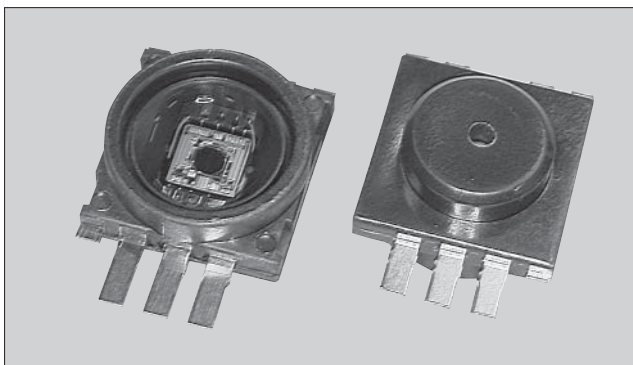
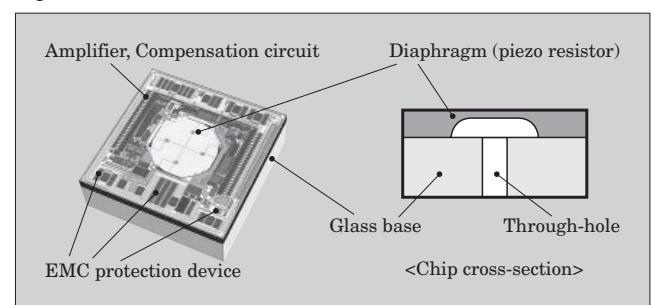


Fig.2 Sensor unit for FTPS



plified. The offset voltage, temperature characteristics are trimmed by the compensation circuits to achieve high output characteristics. The compensation circuit is configured from Digital-to-Analog converters, a shift resistor and an EPROM (electrical programmable read only memory) to store the trimming data. Also, protection devices to protect the circuits from surge voltage and electromagnetic noise from automotive systems such as the igniter or from external sources are also installed in the chip. The above circuits are based on manifold absolute pressure (MAP) sensor technology which has been used since 2002. The glass of the sensor unit and the resin package have a through hole for introducing the reference pressure in order to measure relative pressure. The sensor chip and glass are sealed by an anodic bonding process to prevent leakage with an airtight seal and to relieve stress from the resin package and die bond area.

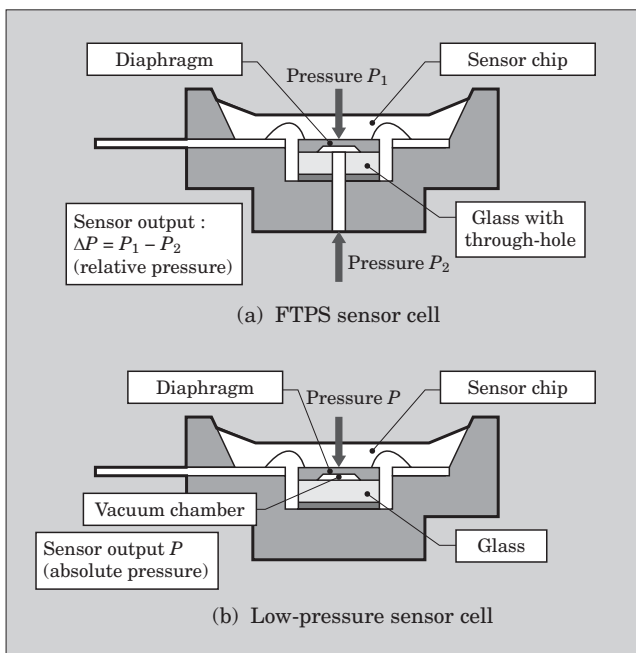
The sensitivity of the FTPS is approximately 200 to 300 mV/kPa, which is about ten times higher than the sensitivity of a MAP sensor.

The chip design for the newly developed FTPS targeted the following improvements.

- (1) Improvement of amplifier linearity and gain in order to obtain higher accuracy and sensitivity
- (2) Design of the diaphragm for high sensitivity and high burst pressure

Figure 3 compares the cross-sections of the FTPS and MAP sensor. The external dimensions of each resin package are the same so that the same production lines can be used in order to reduce machinery cost and production cost.

Fig.3 Cross sections of FTPS sensor cell and low pressure sensor cell structures



4. Design Verification of the FTPS

4.1 Design of the amplifier for high sensitivity and high accuracy

Figure 4 shows a block diagram of the pressure sensor circuit.

The components are based on the MAP sensor's circuit. High sensitivity of the FTPS is achieved by increasing the gain of the amplifier that amplifies the output voltage of the Wheatstone bridge. High accuracy is achieved by improved linearity of the amplifier for the MAP sensor. Figure 5 shows the results of the improved linearity and compares the accuracy of the FTPS with that of a conventional amplifier for a MAP sensor.

4.2 Design of the diaphragm for high sensitivity and high burst pressure

The thickness and diameter of the diaphragm are

Fig.4 Block diagram of output sensor circuit

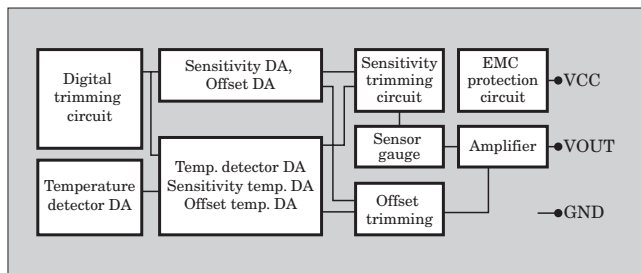
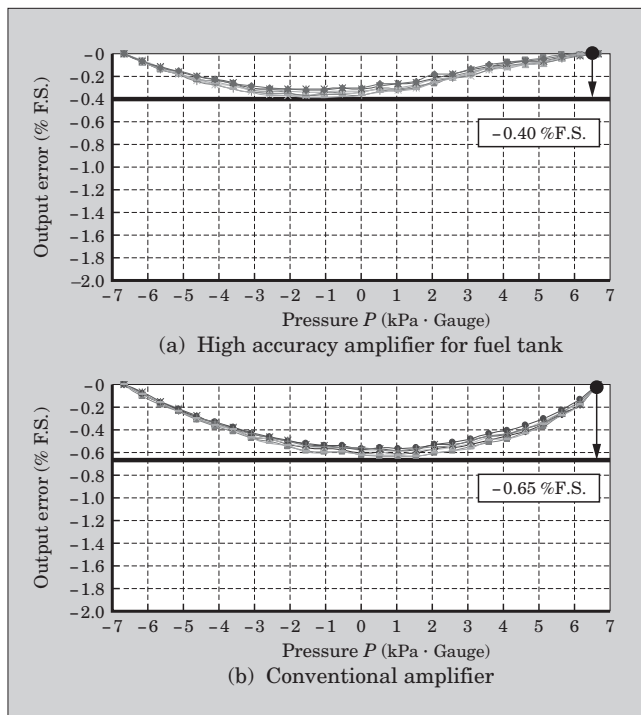


Fig.5 Higher accuracy due to improved linearity of the amplifier



also factors that determine the sensor sensitivity.

Using the finite element method (FEM), we investigated the optimum thickness and diameter of the diaphragm for FTPS. Figure 6 shows the model for FEM analysis of the diaphragm and Fig. 7 shows the FEM analysis results.

4.3 Results of burst pressure test

Burst pressure depends on the thickness of the diaphragm and decreases as the diaphragm becomes thinner. Therefore we evaluated the FTPS diaphragm burst pressure using the thinnest diaphragm within the tolerance for high sensitivity. We found that the diaphragm and the adhesion between the sensor unit and resin cases do not broke at pressure of 500 kPa which corresponds to approximately seventy-five times the 6.6 kPa operating pressure on each surface of the circuit and on the back of the diaphragm.

Fig.6 Diaphragm optimization (FEM analysis model)

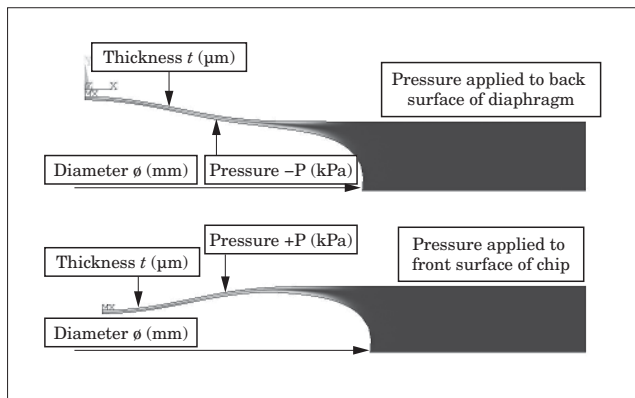
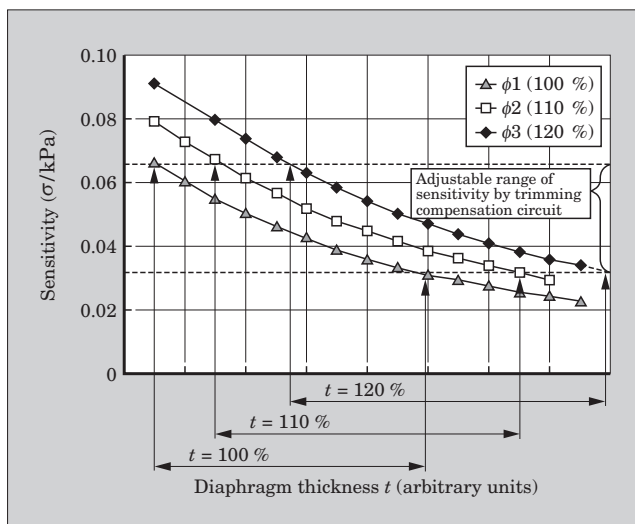


Fig.7 Diaphragm optimization (FEM analysis results)



4.4 Output characteristics of the FTPS

Figure 8 shows the output characteristics of the FTPS when measured at the relative pressure of ± 6.6 kPa. The operating pressure range can be changed from ± 6 kPa to ± 10 kPa (relative pressure) by trimming the compensation circuits on the chip and by changing the thickness of the diaphragm.

4.5 Standard specifications

Table 1 lists the standard specifications of the FTPS.

4.6 Package option and mechanical interface

The FTPS cell package options support a wide range of mounting methods such as a housing type for mounting directly in a fuel tank or a pipe cap on cell package for tube installation.

Fig.8 Pressure vs. output characteristics

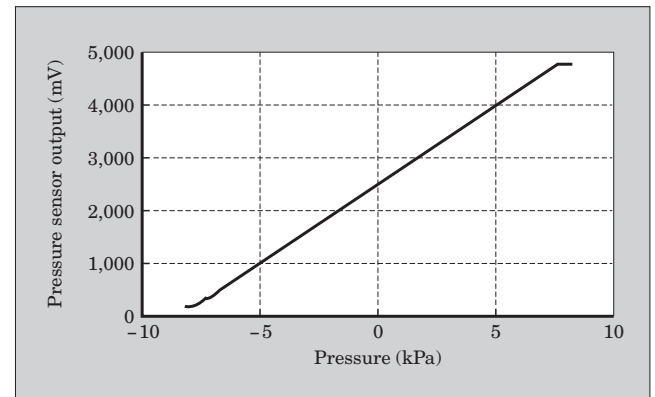


Table 1 FTPS standard specifications

Item	Unit	Specification	Notes
Overvoltage	V	16.5	< 1 min
Proof pressure	kPa	60	
Storage temperature	°C	- 40 to +135	
Operating temperature	°C	- 30 to +125	
Operating pressure	kPa	± 6.66	*1 *2
Output range	V	0.5 to 4.5	
Load resistor	k Ω	Pull-up 300 Pull-down 100	
Diagnostic output voltage	V	< 0.2	*3
	V	> 4.8	*3
Sink current	mA	1	
Source current	mA	0.1	
Pressure error	%F.S.	< 3.0	
Temperature error	Scaling factor	< 1.5	
EMC certified standard	JASO D00-87 / CISPR 25 ISO 11452-2 / ISO 7637		

*1 Relative pressure

*2 Full-scale pressure range trimming is optionally available.

*3 Output voltage when the Vcc or Vout line is open

The diagnostic output voltage depends on the load resistance.

5. Conclusion

Fuji Electric has developed a pressure sensor cell for fuel leak detection that uses a CMOS process-based digital trimming scheme. This paper presented a product overview, discussed considerations relating to the high sensitivity and burst pressure design, and reported the results of a product evaluation. The basic specifications of the newly developed sensor cell are well suited for applications within the pressure range of 6 to 10 kPa (relative pressure), and package options sup-

port a wide range of mounting methods. Automotive regulations for safety and environmental protection will become stricter throughout the world. The marketplace needs for pressure sensors will be increase in the future. Fuji Electric intends to develop new pressure sensors with high accuracy and high performance in order to contribute to the automotive market and protect the environment.

Reference

- (1) Ueyanagi, K. et al, FUJI ELECTRIC REVIEW. Vol.50, No.2, 2004, p.68-70



M-Power 2A Series of Multi-chip Power Devices

Takayuki Shimatoh
Noriho Terasawa
Hiroyuki Ota

1. Introduction

Fuji Electric has developed highly efficient and low-noise proprietary multi-oscillated current resonant circuits for use in switching power supplies. As a custom device for this circuit, Fuji Electric has commercialized the “M-Power 2”, housed in a small package (SIP23) containing a control IC and two power MOS FETs (metal oxide semiconductor field effect transistors), and this device has been well received for use in power supplies for flat panel televisions. As a result of the trend toward increasingly larger sizes of flat panel televisions in recent years, large capacity power supplies (having an output power of approximately 400 W) are being required. To support even larger capacity power supplies, Fuji Electric has developed the M-Power 2A series of devices provided with power MOS FETs having a lower ON-resistance, and featuring improved control IC functionality.

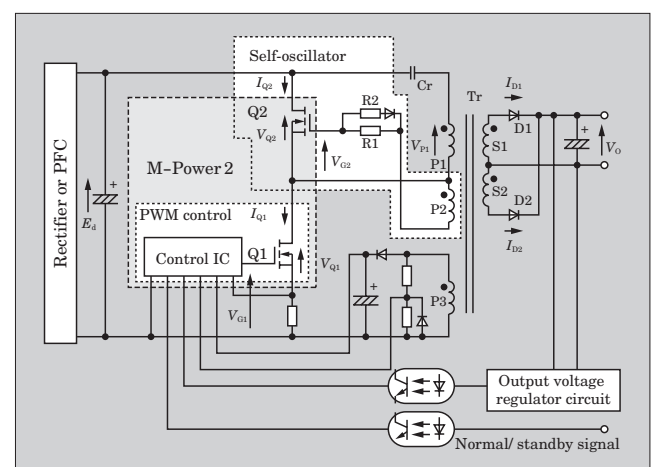
This paper introduces the M-Power 2 series and the M-Power 2A series of multi-chip power devices, and the operating principles of the multi-oscillated current resonant power supply, to which these devices are applied.

2. Operating Principles of the Multi-oscillated Current Resonant Converter

2.1 Circuit configuration

Figure 1 shows the basic circuit configuration of a multi-oscillated current resonant converter in which an M-Power 2 device is used. In the upper and lower arms, the low-side switch Q1 (power MOSFET) is separately-excited (PWM controlled) and is driven by a control IC and the high-side switch Q2 (power MOSFET) is self-excited and is driven by an auxiliary winding P2 of an isolated transformer Tr, and current resonant operation is implemented with a series resonant circuit consisting of the Tr leakage inductance and a resonant capacitor Cr. P2 and the Vcc control winding P3, which supplies power to the control IC, are designed to be tightly coupled to P1, and each generates a voltage proportional to the P1 voltage. However, the P2 voltage has the reverse phase of the P1 voltage.

Fig.1 Basic circuit configuration of the multi-oscillated current resonant converter



2.2 Basic operation

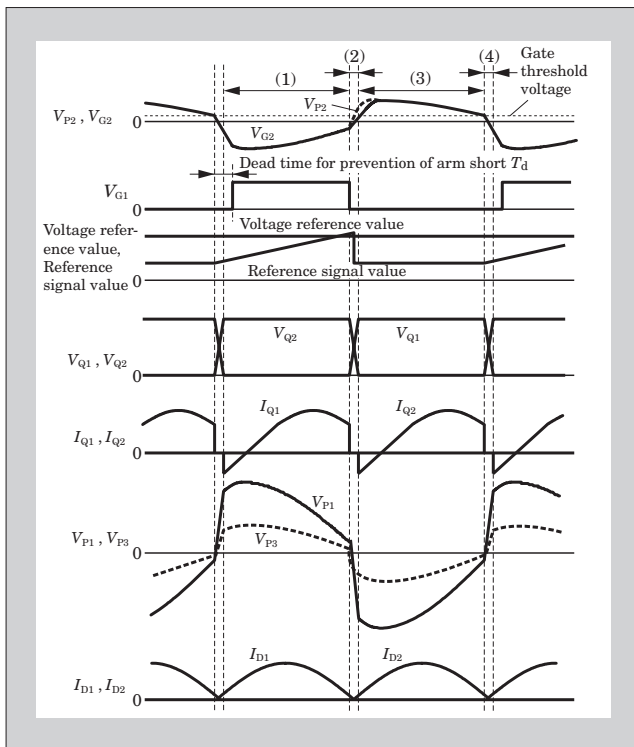
Figure 2 shows the operational timing chart.

During period (1), in the state where Q1 is ON and Q2 is OFF, a current flows through Cr to P1 and supplies power to the load. Output voltage control is implemented by feeding back to the control IC the signal from the output voltage regulator circuit as a voltage reference. The control IC compares the voltage reference to a reference signal value that increases in proportion to the time elapsed since the zero-crossing of V_{P1} (from negative to positive) and performs PWM control of Q1 so that the output voltage becomes constant.

During period (2), when Q1 turns OFF, the polarity of V_{P1} inverts from positive to negative. Current for charging the Q1 output capacitance and current for discharging the Q2 output capacitance flows from Tr, and the Q1 drain voltage rises and the Q2 drain voltage drops.

During period (3), after the discharge is completed, the Q2 body diode begins to conduct. At this timing, ZVS (zero voltage switching) becomes active when Q2 turns ON. The gate voltage turn-on voltage is moderated by a resistance connected to the Q2 gate terminal, and the circuit is set such that ZVS will become active and prevent Q1 and Q2 from both turning ON simulta-

Fig.2 Operational timing chart



neously and a short-circuit current from flowing. Also, with Q2 in an ON state, a current, inverted from that of period (1), flows to P1 and supplies power to the load.

Operation during period (4) is the same as during period (2). Afterwards, the operation returns to period (1), and when discharging is completed, the Q1 body diode begins to conduct. At this timing, ZVS becomes active when Q1 turns ON. After the timing of the negative to positive zero-crossing of V_{P1} is indirectly detected by the P3 voltage, and after the time T_d , dead time for prevention of an arm short, has elapsed, Q1 is turned ON.

2.3 Features

The converter has the following features.

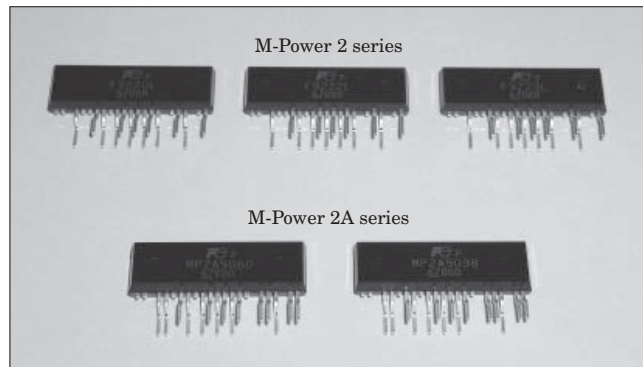
- (1) High efficiency
- (2) Low noise
- (3) No arm-short by lower frequency side operation (the resonant breakaway phenomenon)
- (4) High efficiency during light load operation

Features (1) and (2) above provide the same benefit as the conventional current resonant circuit frequency control method. However, features (3) and (4) are difficult to achieve with the frequency control method, and a significant advantage of the present method is the ability to provide these countermeasures and improvements easily.

3. Overview of the M-Power 2A Series

Figure 3 shows the appearance of the M-Power 2

Fig.3 Appearance of M-Power 2 and M-Power 2A series devices



and M-Power 2A series devices. These devices use the same package construction. The M-Power 2A series features improved control IC functionality, and its pin layout differs from that of the M-Power 2 series.

3.1 Structure

Internally, the M-Power 2A has an all-silicon multi-chip configuration, and the M-Power 2A houses a control IC and two power MOSFETs (Q1 and Q2) in a SIP package having a height of 10 mm and width of 30 mm, which is suitable for application to low-profile power supplies.

3.2 Control IC functions

The control IC, which was developed specially for multi-oscillated control, has some general functions. One is a computation function to control the PWM (pulse width modulation) operation of the Q1 according to the indicated value for the secondary side output voltage. The other is a protection function by latched shutdown against the overcurrent, load short-circuit, overheat, overvoltage and undervoltage lockout. Also, the latched shutdown function of the overcurrent protection and the overheat protection is provided with a timer setting.

3.3 Power MOSFET

The power MOSFET used is a SuperFAP-G series power MOSFET having the characteristics of low-resistance and high switching speed, and aims to reduce loss.

4. Improvements to the M-Power 2A and Differences from the M-Power 2 Series

The improvements to the M-Power 2A and differences from the M-Power 2 series are as listed below.

4.1 Structural improvements

Compared to the lead frame structure of the M-Power 2, the M-Power 2A has a larger mounting area for the power MOSFETs (Q1 and Q2), and enables the mounting of power MOSFETs having lower ON-

resistance (in order to ensure sufficient current capacity, the provision of two main current terminals). As a result, the MP2A5038 (500 V/0.38 Ω) is well suited for application to output switching power supplies of approximately 400 W.

4.2 Control IC function and performance improvements

Table 1 compares the functions of the M-Power 2 and the M-Power 2A.

- (1) Improved output voltage dropout characteristics at sudden change in load

In the case of unloaded burst operation as shown in Fig. 4 for a power supply equipped with an M-Power 2 device, if the load is suddenly changed to a near maximum loaded condition, a phenomenon occurs in which the output voltage drops significantly. The voltage drop occurs because after a sudden load change (from no load to maximum load) during burst operation, even if the output voltage reference value, COMP voltage (FB (feedback) voltage in the case of the M-Power 2A), rises, switching does not restart unless the CB (burst operation frequency) oscillation reaches its lower limit. Thus the M-Power 2A has been devised such that switching restarts soon after the point in time when the FB voltage rises, and therefore there is almost no drop in output voltage, and a dramatic improvement is realized.

- (2) Surge voltage prevention of the overvoltage protection

The M-Power 2's overvoltage protection operates to instantaneously implement a latched shutdown when an excessive voltage (overvoltage) is input. However, it is desired that latched shutdown does not occur for an overvoltage pulse having an extremely narrow width, such as a lightening surge. Therefore, with the

M-Power 2A, the overvoltage protection function is provided with a 270 μ s timer, and does not react to narrow width overvoltage pulses.

- (3) Less resistive loss for overcurrent protection detection

With the M-Power 2 series, overcurrent protection circuit has an operating voltage of 900 mV, the current detection resistance loss increases as the power supply output power increases, and increasing the size of the detection resistor results in greater heat generation. On the other hand, the M-Power 2A has a lower operating voltage of 171 mV, and achieves reduced detection resistance loss. The following improvements have been made in the M-Power 2A.

- (a) The current detection method has been changed from plus to minus, and the influence of the power MOSFET's drive current has been eliminated.
- (b) The current detection terminal is separated from the power MOSFET's source terminal, and an externally attached filter can be designed freely in accordance with the power supply specifications.
- (c) Two GND terminals (PGND and SGND) are provided, the influence of noise on the control IC lessened, and the pattern layout has been made easier to design.
- (4) Built-in compensation circuit for light load burst

Table 1 Functional comparison of M-Power 2 and M-Power 2A

Item	M-Power 2	M-Power 2A
Input power at standby (when $P_o = 0$ W)	0.6 W (burst operation)	0.41 W (burst operation)
	Built-in standby mode	External standby circuit
Switching restart timing	Minimum of CB oscillation	FB voltage reaches V_{thFB}
Dead time for prevention of arm short	Fixed	Adjustable
Circuit to prevent audible noise at light load	External circuit	Built-in
Overvoltage protection (OV)	1 shot latch	Timer latch at 270 μ s
Overcurrent protection (OC)	Plus detection (+900 mV)	Minus detection (-171 mV)
	Timer latch at 100 ms	Timer latch at 36 ms
Short circuit protection (SC)	Plus detection (+1,500 mV)	No function
	1 shot latch	

Fig.4 Schematic drawing of operation at sudden load change

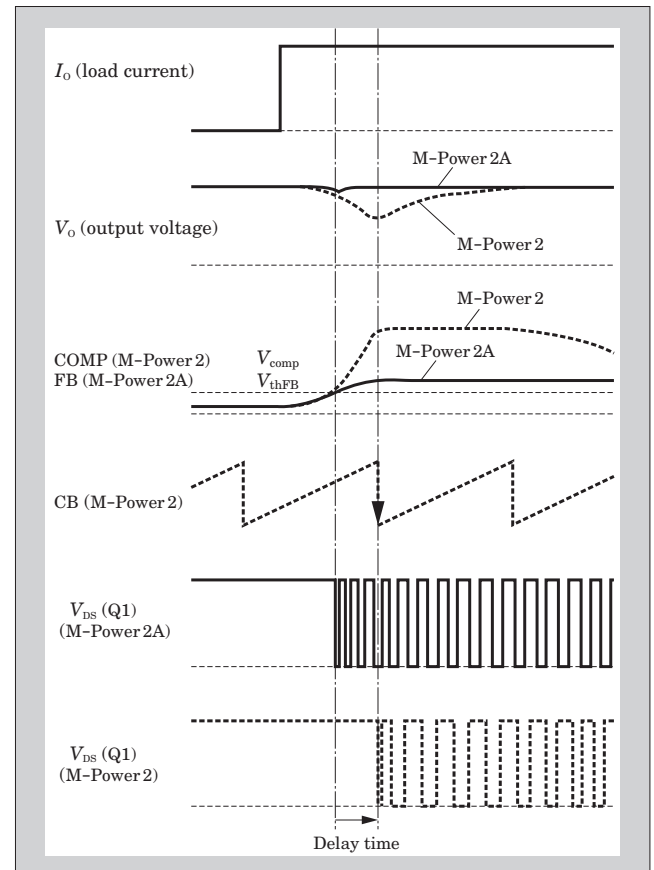


Fig.5 External standby circuit

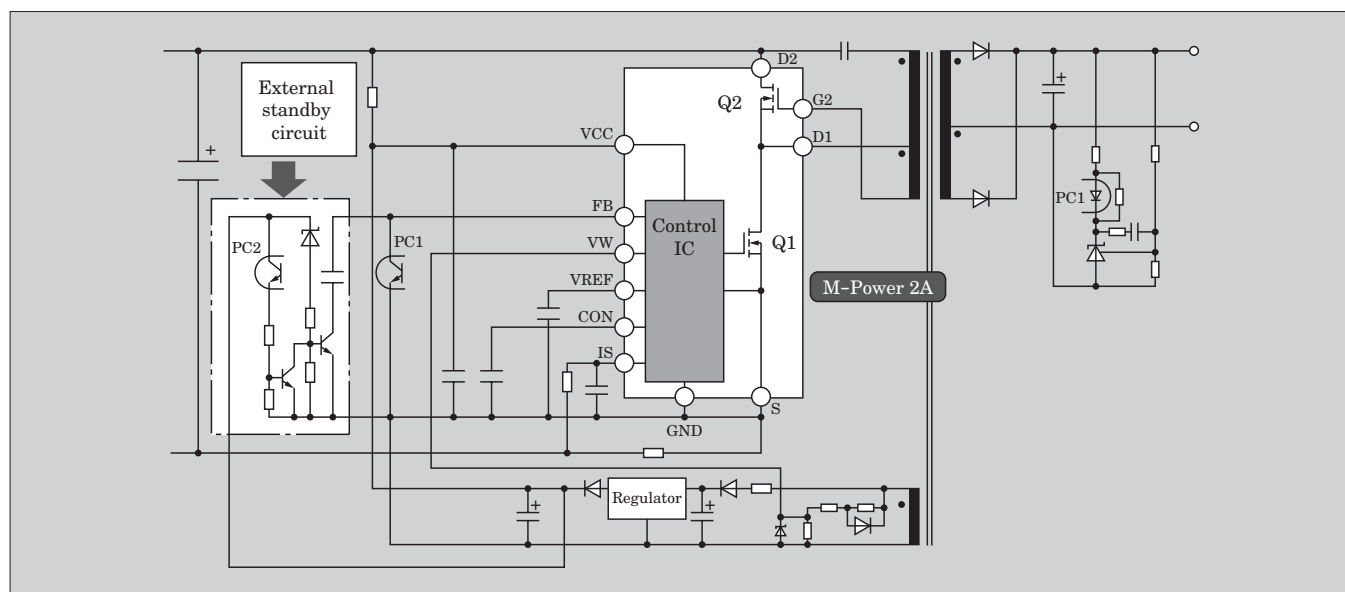


Table 2 Fuji Electric's M-Power 2A series product lineup

Model name	MOSFET (Q1, Q2)		Control IC		Package
	V_{DS}	$R_{DS(ON)}$	$V_{CC(ON)}$	$T_j(ON)$	
MP2A5038	500 V	0.38 Ω	16.5 V	125 to 150°C	SIP23
MP2A5050		0.50 Ω			
MP2A5060		0.60 Ω			
MP2A5077		0.77 Ω			
MP2A5100		1.0 Ω			
MP2A5135		1.35 Ω			

operation

With the M-Power 2, the operation is burst during a light load, and in cases where an audible burst operation sound from Tr creates a problem, it is recommended that a circuit be attached externally to provide a solution. On the other hand, with the M-Power 2A, a compensation circuit for burst operation is built-in, thereby enabling a reduction in the number of externally attached components.

(5) Reduced power consumption of control IC

The M-Power 2 has a built-in standby function, but the M-Power 2A eliminates this function in order to reduce the consumption of electrical power by the control IC. However, in the case where a standby function is required in one converter, a standby function circuit can be attached externally. (See Fig. 5.)

5. Conclusion

This paper has introduced the newly developed M-Power 2A series of products that feature an improved control IC for power supplies in flat panel televisions and the like (Table 2). Accordingly, the M-Power 2A series of devices are well suited for application to large capacity power supplies for use in large screen flat panel televisions and the like. In the future, Fuji Electric plans to expand the product lineup to support various other requests. Fuji Electric also intends to strive to develop power supply systems and to commercialize custom power devices in order to support requests for even more sophisticated power supplies.

Multi-output PDP Scan Driver IC

Naoki Shimizu
Hideto Kobayashi

1. Introduction

Over the past several years, driven by advances in PDP (plasma display panel) and LCD (liquid crystal display) TV technology, flat-screen TVs have rapidly become popular in the market for home-use televisions. The market had previously been divided among large-screen PDP TVs and small-screen LCD TVs, but LCD TVs have recently entered the large-screen market, and competition with PDP TVs is intensifying. Also, with the increase in terrestrial digital broadcasts, and the greater popularity of such products as game devices and DVDs (digital versatile disks), there is demand for not only larger screen displays, but also for higher picture quality, lower cost and lower power consumption.

The peripheral circuitry accounts for a large percentage of the cost of PDPs, and requests are intensifying, year after year, for lower cost driver ICs for driving the PDPs. Since the driver ICs also control the emission of light from the panel, the driver IC performance directly affects the PDP performance. Consequently, lower cost and higher performance are continuously requested of the multiple driver ICs used in a panel.

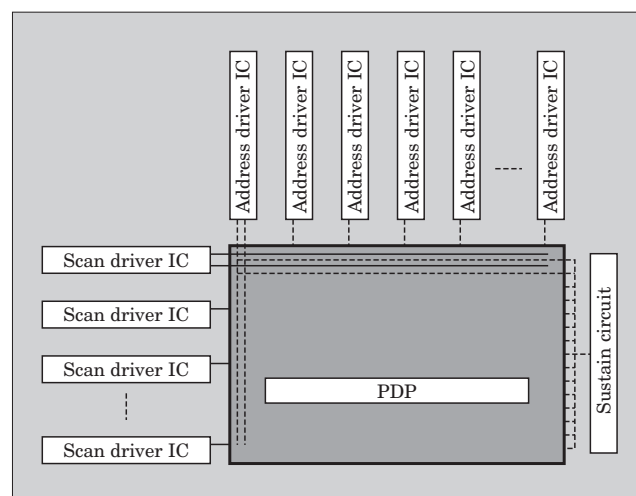
There are two types of PDP driver ICs, scan driver ICs that select scan lines and address driver ICs that select data. Fuji Electric is developing both of these types of IC drivers. This paper introduces a 96-bit scan driver IC developed with the aim of increasing brightness and reducing cost.

2. Features of PDP Scan Driver ICs

A PDP is constructed from a rare gas mixture of Ne, Xe, or the like, encapsulated between two overlapping glass panels on which are formed an electrode matrix consisting of a horizontal arrangement of sustain electrodes, for emitting, and a vertical arrangement of address electrodes, for selectively addressing display data. The intersections of the address electrodes and sustain electrodes demarcate a single PDP cell.

The cell to be displayed is selected by opposing discharges between the address electrodes and the sustain electrodes, and surface discharge is performed among the sustain electrodes. The UV rays generated

Fig.1 PDP module drive circuit



by such discharge excite fluorescent material in each cell, causing light to be emitted.

Figure 1 shows the configuration of a PDP module. Scan driver ICs drive horizontal electrodes in the panel, and simultaneously control all the discharge cells within the panel. The number of ICs used varies according to the type of the panel. Typically, a HD (high definition) panel contains at least 720 vertical pixels which configure the screen, and uses 12 conventional scan driver ICs which has 64 outputs. Also, panels having $1,920 \times 1,080$ pixels for displaying the intricate detail of a high vision broadcast are known as full-HD panels. A panel that supports full-HD (having at least 1,080 vertical pixels) must use 18 conventional scan driver ICs which has 64 outputs.

3. PDP Scan Driver IC Technology

3.1 Device process technology

Scan driver ICs use the SOI (silicon on insulator) method of dielectric isolation technology. Because the isolated device area can be made small without any restrictions on the device, this method is optimal in terms of cost and performance for scan driver ICs that feature a high breakdown voltage, large current and multiple outputs. In a multi-output scan driver IC, the

output circuit area occupies 50 % or more of the entire chip area, and therefore in order to reduce cost, the most effective means for reducing the IC chip area is to reduce the output circuit area. Thus, a scan driver IC which requires a large current flow uses an IGBT (insulated gate bipolar transistors) capable of a large current flow even in a small area, instead of a MOS (metal oxide semiconductor). Fuji Electric's newly developed scan driver ICs have a higher breakdown voltage than conventional scan driver ICs, and are equipped with a low ON-resistance SOI-IGBT device. The lower ON-resistance makes it possible to reduce the amount of heat generated during operation, and the higher breakdown voltage supports higher brightness.

3.2 Circuit technology

Figure 2 shows the main operation and output stage circuit of a scan driver IC. A PDP uses a reset period, an address period, and a sustain period to display a single screen. The main operation of the scan driver IC consists of address and sustain operations, and is described simply below.

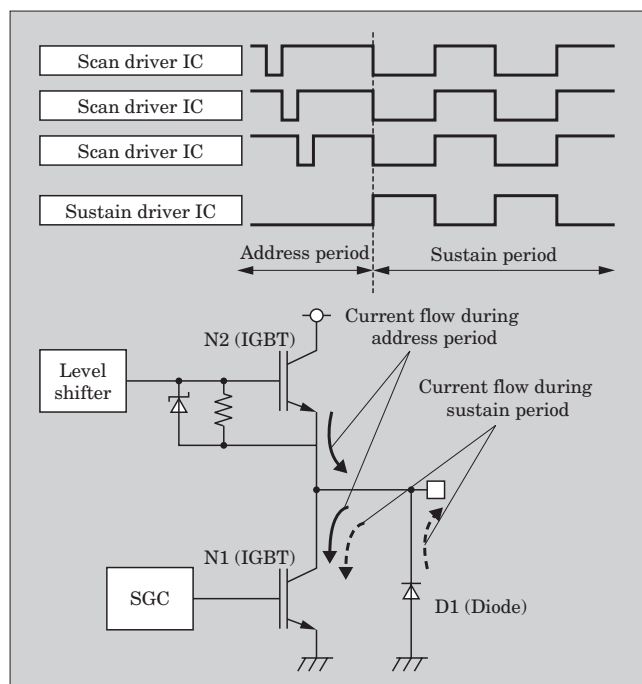
(1) Reset period

In the reset period, a pulse of approximately 350 V is applied so that wall charge can be generated stably during the address period. The applied voltage causes a priming discharge to occur, and wall charge to be removed.

(2) Address period

In the address period, cells are selected or non-selected according to a combination of address driver IC pulses and scan driver IC pulses. When a cell is selected, N1 (IGBT) turns ON, and when de-selected, N2 (IGBT) turns ON and outputs a waveform. A selected

Fig.2 Scan driver IC operation



cell flows a large current through N1 (IGBT) and performs a preliminary discharge. At this time, a voltage of approximately 70 V is applied to the address driver ICs, and for each scan line, a current of at least 1 A flows to a scan driver IC.

(3) Sustain period

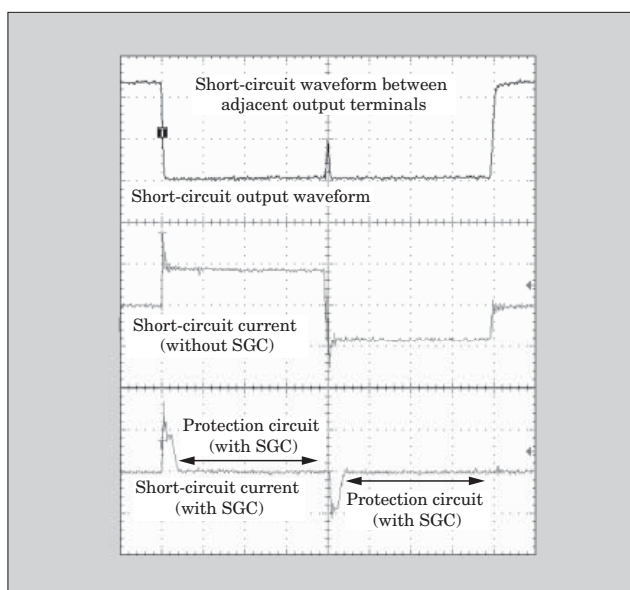
In the sustain period, a voltage of approximately 180 V is applied alternately to the sustain circuit, and the repeated application of pulses causes cells selected during the address period to sustain their discharge. The discharge current is supplied from both N1 (IGBT) and D1 (diode), and a gradated display is implemented according to the number of repeated discharges.

3.3 Smart gate control (SGC) technology

A problem associated with IGBTs is that if a large current is output continuously, latch-up may occur and cause the device to become damaged. In particular, in order to reduce cost, if a device is shrunk and the current density increased, then the device becomes susceptible to damage. One conceivable cause would be an abnormal discharge due to an overload short-circuit condition or abnormal operation such as in the case of short-circuited output terminals. Modifying a device so that there will be no damage when an abnormal operation occurs results in a larger device area and higher cost. Therefore, a SGC (smart gate control) circuit, capable of outputting a large current during a discharge period when current is needed and limiting the current during a discharge period when current is unnecessary, was designed and used in practical applications⁽¹⁾. Since the SGC operation is controlled synchronously with a clock signal, the control circuits can be shared for a multi-output device and the control circuits can be miniaturized.

Figure 3 shows waveforms in the case where adja-

Fig.3 Short-circuit waveforms between adjacent output terminals



cent output terminals have been short-circuited. During a short-circuit condition in the case where SGC technology is not utilized, current will continue to flow and the heat generated as a result of the increased duration of the short-circuit and the rise in voltage will cause damage. However, in cases where SGC technology is utilized, the current flow is stopped after a fixed time has elapsed, and therefore if the short-circuit has a long duration, damage will not occur even if the voltage rises up to a certain level, and therefore, the current density of the device can be increased to reduce the device size. The SGC makes it possible to extend the time until short-circuit damage occurs, and by switching the device OFF before the occurrence of short-circuit damage, a short-circuit will not cause any damage to occur.

4. Application to a PDP Scan Driver IC (FD3298F)

As PDP TVs achieve larger screen sizes, higher resolution and lower cost, driver ICs are being requested to have higher breakdown voltage, larger current and lower cost. In response to these requests, and focusing on multi-output capability, Fuji Electric has increased the breakdown voltage without increasing the device size to develop a 96-bit scan driver IC that enables the number of scan driver ICs used to be reduced, from 12 (previously) to 8, in a HD panel as shown in Table 1. Also, in a full-HD panel, cost reductions can be realized by reducing the number of ICs used from 18 64-bit ICs to 12 96-bit ICs. Fuji Electric's 96-bit scan driver IC, FD3298F, is introduced below.

4.1 Features

Main features of the FD3298F are listed below.

- (1) 96-bit bi-directional shift register (with 15 MHz clear function)
- (2) 180 V absolute maximum rating (supply voltage for output), 7 V absolute maximum rating (supply voltage for logic)
- (3) Power output supply voltage: 30 V to 150 V
- (4) 5 V supply for logic
- (5) Driver output current: $-0.4\text{ A}/+1.4\text{ A}$ (source/sink)
- (6) Diode output current: $-1.4\text{ A}/+1.2\text{ A}$ (source/sink)
- (7) 128-pin TQFP with exposed pad (E-PAD)

4.2 Circuit configuration

Figure 4 shows a block diagram of the FD3298F. The circuit is configured from a 96-bit bi-directional shift register circuit, a 96-bit latch circuit, data select

circuits, and a 96-bit output circuit. So that the output circuit can charge and discharge the discharge cells in the panel, a totem pole output circuit configured from two devices having a high breakdown voltage is used in the output circuit. In order to prevent malfunction, Schmitt circuits are connected to the shift register input terminals, with the exception of the A/B signal terminal that determines the direction of the shift register. Also, the logic output is a trailing edge output with respect to the clock signal.

4.3 Comparison with a conventional IC

Figure 5 compares the chip size of a conventional

Fig.4 FD3298F block diagram

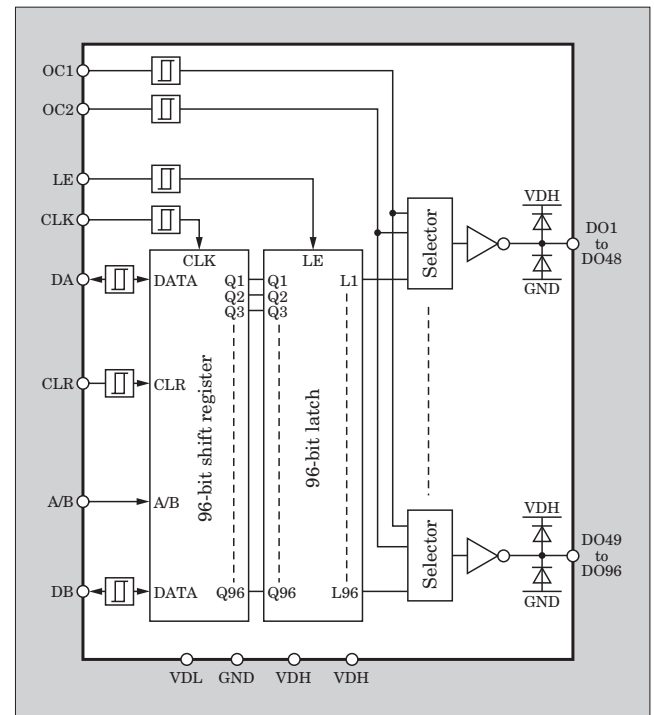


Fig.5 Die size comparison of FD3298F and conventional scan driver IC

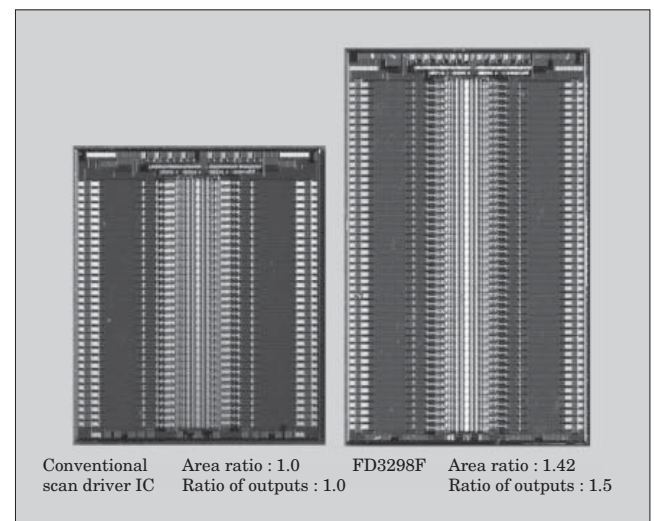
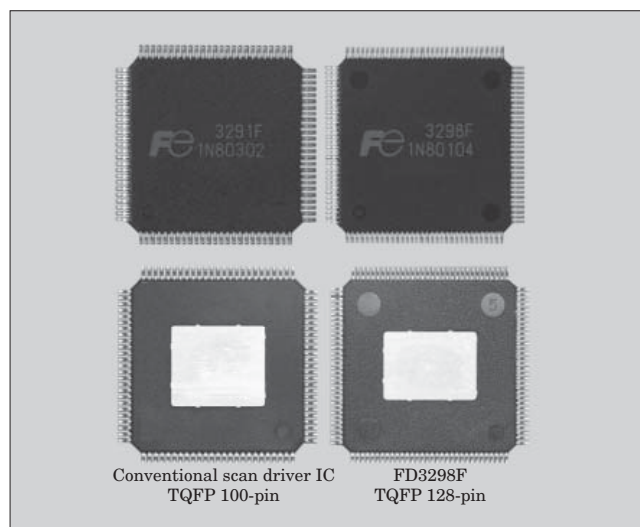


Table 1 Number of scan driver ICs used

Resolution	Scan lines	64ch IC use number	96ch IC use number
SD (VGA)	480	8	6
HD (XGA)	over 720	12	8
Full HD	1,080	18	12

Fig.6 External appearance of FD3298F and conventional packages



scan driver IC and the FD3298F. The chip size of the FD3298F is 1.42 times that of a conventional 64-bit scan driver IC, but the number of bits is 1.5 times greater, and since the number of chips used will decrease, the cost will lower than in the case of conventional scan driver ICs.

Figure 6 shows the external appearance of the package. The conventional IC package uses a TQFP 100-pin (E-PAD) package, but since the FD3298F has a 96-bit output, the FD3298F uses a TQFP 128-pin (E-PAD) package. The increase in the number of output bits creates a problem of more heat generated, but by reducing the ON-resistance to a value lower than that of the conventional scan driver IC, the generation of heat during operation is reduced, and by increasing the number of E-PADs and pins, heat is dissipated more efficiently from the package.

5. Conclusion

Fuji Electric's PDP scan driver IC, FD3298F, which was developed with the aim to achieve higher breakdown voltage and lower cost has been introduced.

Fuji Electric intends to continue to develop device technology, circuit technology and process technology for scan driver ICs in response to marketplace and panel manufacturer's requests.

Reference

- (1) Kobayashi, H. et al. PDP Scan Driver IC with Smart Gate Controlled IGBTs. IDW'04. PDP3-3.

A 2nd Generation Micro DC-DC Converter

Isao Sano
Yoshikiyo Usui
Tomonori Seki

1. Introduction

While miniaturization of cell phones, digital still cameras, portable music players and other types of portable electronic equipment is being accelerated, lower current consumption is being required in order to enable longer continuous usage of batteries. For this purpose, the power supply control ICs installed in such equipment are required to have a smaller footprint and to operate at higher efficiency to the extent possible.

In response to these requirements, micro DC-DC converters that integrate a control IC and an inductor have been developed and commercialized.

The originally developed prototype had a monolithic structure in which a thin film inductor was formed on the control IC, and although a thinner package was realized, problems remained with the product size and efficiency.

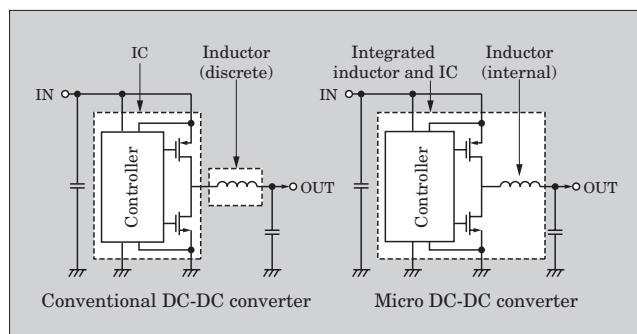
Thereafter, using a structure in which a dual-purpose substrate on which an inductor is mounted is connected to a control IC by flip chip bonding, the problems associated with the prototype were solved and a 1st generation product was commercialized.

This paper introduces Fuji Electric's newly developed FB6831J, a 2nd generation micro DC-DC converter that realizes an even smaller size.

2. Features

The micro DC-DC converter, as shown in Fig. 1, achieves a smaller size as well as a fewer components

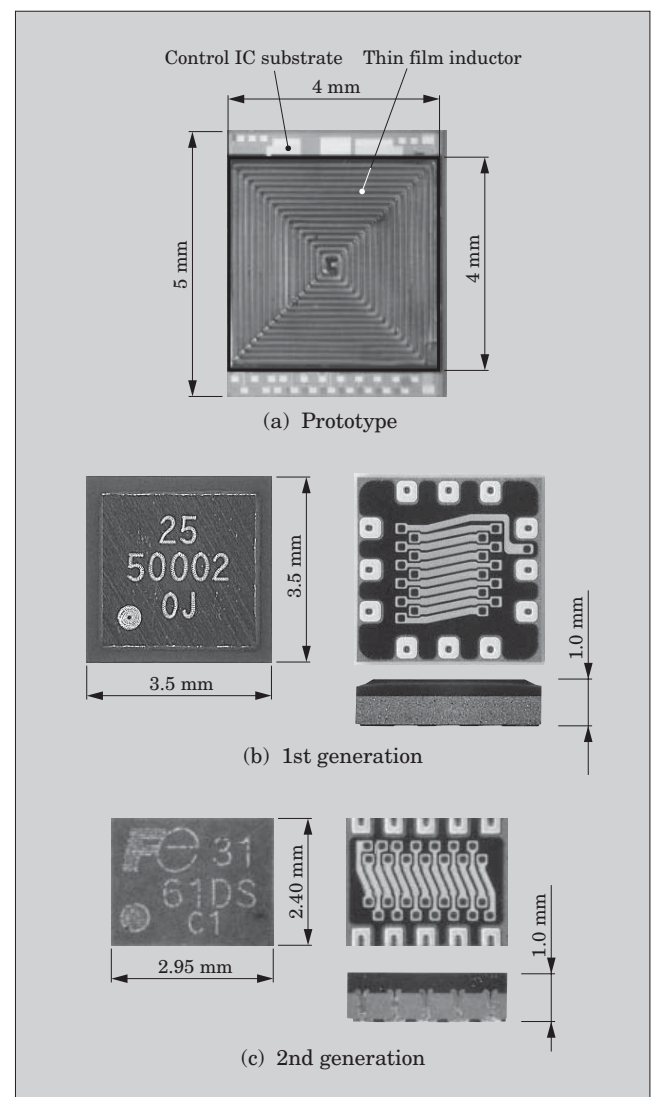
Fig.1 Micro DC-DC converter configuration



configuration by integrating the discrete inductor, selectable by the user according to the application in a conventional DC-DC converter, with the control IC. The concept of the micro DC-DC converter is to provide a DC-DC converter that is as easy to use as a LDO (low drop out) regulator.

Figure 2 shows the external appearance of the mi-

Fig.2 External appearance of micro DC-DC converter



cro DC-DC converter. The product footprint has been reduced by approximately 40 % with each successive generation.

The FB6831J is a micro DC-DC converter that has step-down output voltage from the input voltage of a single-cell Li-ion battery. The FB6831J has a maximum output current of 500 mA.

Main features of the FB6831J are listed below.

- (1) External dimensions: As shown in Fig. 2(c), the FB6831J realizes dimensions of 2.95 mm × 2.40 mm, and a thickness of 1 mm (typ).
- (2) Package: As shown in Fig. 2(c), by using a CSM (chip size module) having ten terminals arranged on two sides, a micro DC-DC converter module of almost the same size as the die size is realized
- (3) Terminal configuration: The use of a SON (small outline non-lead) structure in which the terminals do not extend from the exterior of the package (PKG) contributes to the smaller footprint.
- (4) Inductor: $L = 1.25 \mu\text{H}$ (300 mA), $R_{dc} = 0.1 \Omega$
As shown in Fig. 2(c), the inductor structure has the same toroidal shape as the 1st generation converter, but the terminals are arranged on two sides. Further, by increasing the percentage of area occupied by the inductor coil pattern, the module area size has been reduced down to 60 % while an inductance value of 75 % that of the 1st generation converter is obtained. Using a thick film for the coil conductor has achieved an approximate 50 % reduction in R_{dc} . Moreover, by selecting a ferrite-based substrate material with lower core loss, the design was optimized to resist magnetic saturation.

- (5) Protection circuit: The FB6831J is equipped with an internal protection circuit to protect against such abnormal conditions as shorting to ground, chip overheating and UVLO (under-voltage lock out), and also to provide overcurrent protection. When an abnormal condition is detected, the protection circuit suspends operation of the chip. Setting the CE terminal to an L-level voltage releases the protection state, and setting the terminal to an H-level voltage returns the chip to its normal operation.
- (6) Switching frequency: 2.5 MHz
High-speed operation is realized through optimized design of the dead time control, driver circuits, high-speed comparators, and oscillation circuits.
- (7) Low current consumption: Standby mode: 1 μA , Operating mode: 300 μA
Each circuit cell was designed for low current consumption to realize the low level of current consumption required in portable electronic equipment.

The main electrical characteristics of the FB6831J are listed in Table 1.

3. Module Technology for the Micro DC-DC Converter

The structures of the prototype, 1st generation and 2nd generation models are compared in Table 2. The 2nd generation micro DC-DC converter assembly uses low loop wire bonding to realize a product thickness of 1 mm (typ).

Table 1 Main electrical characteristics

Item	Symbol	Condition	min	typ	max	Unit
Power supply voltage	V_{DD}		2.7	3.6	5.5	V
Current consumption	I_{VDD1}	VDD Pin CE = L	–	0.1	1	μA
	I_{VDD2}	VDD Pin CE = H, Unloaded	60	80	100	μA
	I_{PVDD1}	PVDD Pin CE = L	–	0.1	1	μA
	I_{PVDD2}	PVDD Pin CE = H, $I_{OUT} = 300 \text{ mA}$ $V_{OUT} = 1.5 \text{ V}$	–	145	165	mA
Output voltage range	V_{OUT}	$I_{load} = 0 \text{ to } 500 \text{ mA}$	0.8	–	$V_{IN} - 0.7$	V
Output voltage accuracy	V_{OUTA}	$I_{load} = 0 \text{ to } 500 \text{ mA}$, $V_{OUT} = 1.5 \text{ V}$	–3	–	3	%
Output ripple voltage	V_{ripple}	$V_{OUT} = 1.5 \text{ V}$, $I_{load} = 300 \text{ mA}$, Capacitor ESR < 100 m Ω	–	–	40	mVp-p
		$V_{OUT} = 1.5 \text{ V}$, $I_{load} = 500 \text{ mA}$, Capacitor ESR < 100 m Ω	–	–	50	mVp-p
Maximum efficiency	η_1	$V_{OUT} = 1.8 \text{ V}$, $I_{load} = 200 \text{ mA}$	–	90	–	%
	η_2	$V_{OUT} = 1.5 \text{ V}$, $I_{load} = 200 \text{ mA}$	–	85	–	%
Oscillation frequency	f_{OSC}	$I_{OUT} = 50 \text{ mA}$	2.3	2.5	2.7	MHz
UVLO ON threshold voltage	V_{UVLH}		2.3	2.4	2.5	V
UVLO OFF threshold voltage	V_{UVLL}		2.2	2.3	2.4	V

Table 2 Structural comparison

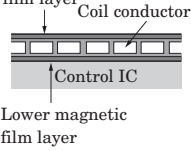
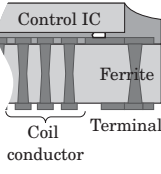
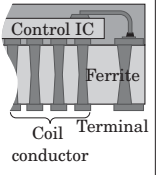
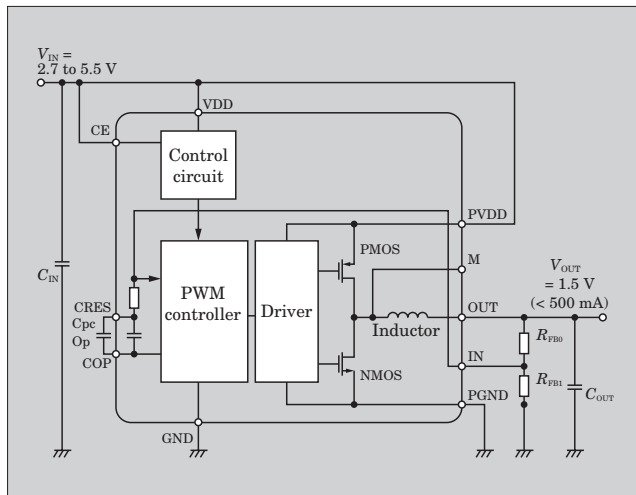
	Prototype	1st generation	2nd generation
Assembly structure	Monolithic structure	Flip chip bonding	Wire bonding
Cross section			

Fig.3 FB6831J block diagram



In the 1st generation assembly that used flip chip bonding, control IC pads were arranged at fixed locations, and therefore the chip size of the control IC could not be reduced due to the constraint of the inductor size. The newly developed assembly uses wire bonding, which allows for a greater degree of freedom in the positioning of the control IC pads and in determining the chip size, enabling cost-effective optimal chip design. On the other hand, because wire bonding has higher wire resistance than flip chip bonding, multiple wires are installed for the large current, low impedance terminals. After the wire bonding has been completed, the control IC surface is coated with a liquid resin, and the inductor substrate is diced to form the individual micro DC-DC converters.

4. Application Circuit

Figure 3 shows a block diagram and Fig. 4 shows an example application circuit of the FB6831J. Because this product is equipped with an internal inductor, an output MOS (metal oxide semiconductor) and a phase compensation circuit, the only external parts are I/O capacitors and voltage-setting resistors, to configure a buck converter, FB6831J contributes greatly to the

Fig.4 Example application circuit

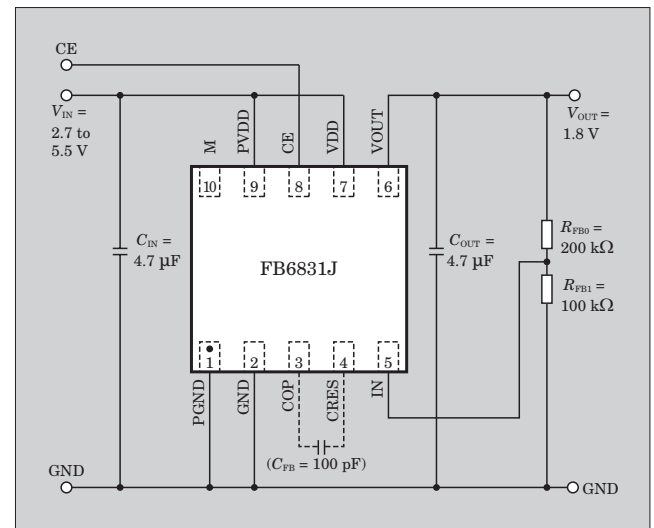
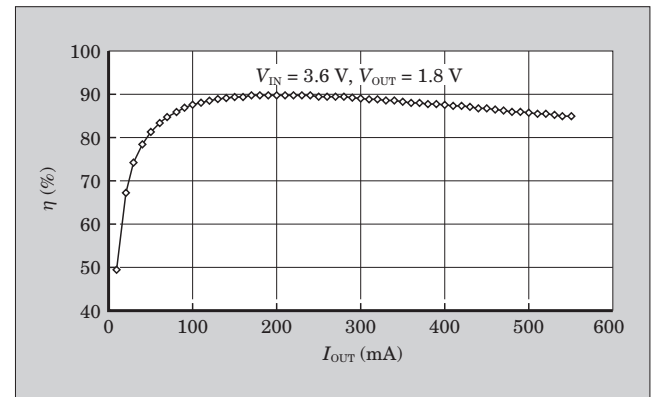


Fig.5 FB6831J efficiency



miniaturization of portable electronics equipment.

The newly developed FB6831J incorporates the following innovations to realize higher efficiency.

- (1) Control circuit (IC): Optimized dead time, lower current consumption of each block, optimized oscillation frequency
- (2) Output MOS (device) size: Size has been optimized such that conductive loss, low gate charge loss, and low drain capacitance loss are a minimum at the switching frequency.
- (3) Inductor: Selection of substrate material that reduces core loss. Terminal arrangement that optimizes the coil pattern area

An actual measurement example of efficiency is shown in Fig. 5.

High efficiency of 90 % is realized at $V_{IN} = 3.6$ V, $V_{OUT} = 1.8$ V and $I_{OUT} = 200$ mA.

Use of the newly developed and commercialized FB6831J enables the construction of a DC-DC converter system enabling a smaller and thinner assembled device, and longer battery life.

5. Conclusion

The FB6831J has been introduced as a 2nd generation DC-DC converter module for use with a single-cell Li-ion battery in applications mainly in portable electronic equipment including cell phones, digital still cameras and the like.

In the future, Fuji Electric plans to add to its product lineup a micro DC-DC converter that supports various input voltages and output voltages. Fuji Electric also intends to continue to develop inductor

material capable of ensuring the required inductance values even when the physical size of the inductor is small, and to develop a low $R_{on}Q_g$ device having low gate charge loss and low drain capacitance loss even when the switching frequency is high to realize higher efficiency and smaller size.

Reference

- (1) Hayashi, Z. et al. High-Efficiency DC-DC Converter Chip Size Module With Integrated Soft Ferrite. THE 2003 INTERNATIONAL MAGNETICS CONFERENCE (INTERMAG 2003).



Global Network



■ : Representative Office ● : Sales Bases ◆ : Manufacturing Bases

AMERICA

- **FUJI ELECTRIC CORP. OF AMERICA**
USA
Tel : +1-201-712-0555 Fax : +1-201-368-8258
- ◆ **FUJI ELECTRIC DEVICE TECHNOLOGY AMERICA INC.**
USA
Tel : +1-732-560-9410 Fax : +1-732-457-0042
- ◆ **FUJI HI-TECH, INC.**
USA
Tel : +1-510-651-0811 Fax : +1-510-651-9070

EU

- **FUJI ELECTRIC HOLDINGS CO., LTD.**
Erlangen Representative Office
GERMANY
Tel : +49-9131-729613 Fax : +49-9131-28831
- **FUJI ELECTRIC FA EUROPE GmbH**
GERMANY
Tel : +49-69-6690290 Fax : +49-69-6661020
- **FUJI ELECTRIC DEVICE TECHNOLOGY EUROPE GmbH**
GERMANY
Tel : +49-69-6690290 Fax : +49-69-6661020
- ◆ **FUJI ELECTRIC FRANCE S.A.**
FRANCE
Tel : +33-4-73-98-26-98 Fax : +33-4-73-98-26-99

ASIA

East Asia

- **FUJI ELECTRIC HOLDINGS CO., LTD.**
China Representative Office (Shanghai)
CHINA
Tel : +86-21-5496-3311 Fax : +86-21-5496-0189
- **FUJI ELECTRIC HOLDINGS CO., LTD.**
China Representative Office (Beijing)
CHINA
Tel : +86-10-6505-1264 Fax : +86-10-6505-1851
- **FUJI ELECTRIC FA (SHANGHAI) CO., LTD.**
CHINA
Tel : +86-21-5496-1177 Fax : +86-21-6422-4650
- ◆ **FUJI ELECTRIC (CHANGSHU) CO., LTD.**
CHINA
Tel : +86-512-5284-5642 Fax : +86-512-5284-5640
- ◆ **FUJI GE DRIVES (WUXI) CO., LTD.**
CHINA
Tel : +86-510-8815-2088 Fax : +86-510-8815-9159
- ◆ **FUJI ELECTRIC DALIAN CO., LTD.**
CHINA
Tel : +86-411-8762-2000 Fax : +86-411-8762-2030
- ◆ **SHANGHAI FUJI ELECTRIC SWITCHGEAR CO., LTD.**
CHINA
Tel : +86-21-5718-1495 Fax : +86-21-5718-5745
- ◆ **SHANGHAI FUJI ELECTRIC TRANSFORMER CO., LTD.**
CHINA
Tel : +86-21-5718-1495 Fax : +86-21-5718-5745

- ◆ **DALIAN FUJI BINGSHAN VENDING MACHINE CO., LTD.**
CHINA
Tel : +86-411-8730-5902 Fax : +86-411-8730-5911
- **DALIAN JIALE VENDING MACHINE OPERATION CO., LTD.**
CHINA
Tel : +86-411-8665-0277 Fax : +86-411-8596-2732
- ◆ **HANGZHOU FUJI REFRIGERATING MACHINE CO., LTD.**
CHINA
Tel : +86-571-8821-1661 Fax : +86-571-8821-0220
- ◆ **FUJI ELECTRIC (SHENZHEN) CO., LTD.**
CHINA
Tel : +86-755-2734-2910 Fax : +86-755-2734-2912
- **FUJI ELECTRIC FA (ASIA) CO., LTD.**
HONG KONG
Tel : +852-2311-8282 Fax : +852-2312-0566
- **FUJI ELECTRIC DEVICE TECHNOLOGY HONG KONG CO., LTD.**
HONG KONG
Tel : +852-2664-8699 Fax : +852-2664-8040
- **FUJI ELECTRIC SYSTEMS CO., LTD.**
Taipei Representative Office
TAIWAN
Tel : +886-2-2561-1255 Fax : +886-2-2561-0528
- **FUJI ELECTRIC TAIWAN CO., LTD.**
TAIWAN
Tel : +886-2-2515-1850 Fax : +886-2-2515-1860
- **FUJI ELECTRIC FA (TAIWAN) CO., LTD.**
TAIWAN
Tel : +886-2-2370-2390 Fax : +886-2-2370-2389
- ◆ **ATAI FUJI ELECTRIC CO., LTD.**
TAIWAN
Tel : +886-3-321-3030 Fax : +886-3-321-7890
- **FUJI ELECTRIC FA KOREA CO., LTD.**
KOREA
Tel : +82-2-780-5011 Fax : +82-2-783-1707

Southeast Asia

- **FUJI ELECTRIC SYSTEMS CO., LTD.**
Bangkok Representative Office
THAILAND
Tel : +66-2-308-2240 Fax : +66-2-308-2242
- **FUJI ELECTRIC SYSTEMS CO., LTD.**
Jakarta Representative Office
INDONESIA
Tel : +62-21-572-4281 Fax : +62-21-572-4283
- ◆ **FUJI ELECTRIC (MALAYSIA) SDN. BHD.**
MALAYSIA
Tel : +60-4-403-1111 Fax : +60-4-403-1496
- ◆ **FUJI ELECTRIC PHILIPPINES, INC.**
PHILIPPINES
Tel : +632-844-6183 Fax : +632-844-6196
- **FUJI ELECTRIC SINGAPORE PRIVATE LTD.**
SINGAPORE
Tel : +65-6535-8998 Fax : +65-6532-6866
- ◆ **FUJI ELECTRIC FA SINGAPORE PRIVATE LTD.**
SINGAPORE
Tel : +65-6533-0010 Fax : +65-6533-0021

